Molecular Therapy
Oncolytics
Original Article

Nanobody-derived bispecific CAR-T cell therapy enhances the anti-tumor efficacy of T cell lymphoma treatment

Baijin Xia,[1,2,3] Keming Lin,[3] Xuemei Wang,[3] FeiLi Chen,[4] Mo Zhou,[3] Yuzhuang Li,[3] Yingtong Lin,[3] Yidan Qiao,[3] Rong Li,[3] Wanying Zhang,[3] Xin He,[3] Fan Zou,[1,2,5] Linghua Li,[6] Lijuan Lu,[7] Cancan Chen,[8] WenYu Li,[4] Hui Zhang,[3] and Bingfeng Liu[3]

[1]Guangdong Cardiovascular Institute, Guangdong Provincial People's Hospital, Guangdong Academy of Medical Science, Guangzhou 510080, China; [2]Medical Research Institute, Guangdong Provincial People's Hospital, Guangdong Academy of Medical Science, Southern Medical University, Guangzhou 510080, China; [3]Institute of Human Virology, Key Laboratory of Tropical Disease Control of the Ministry of Education, Guangdong Engineering Research Center for Antimicrobial Agent and Immunotechnology, Zhongshan School of Medicine, Sun Yat-sen University, Guangzhou, Guangdong 510080, China; [4]Lymphoma Department, Guangdong Provincial People's Hospital, Guangdong Academy of Medical Sciences, Southern Medical University, Guangzhou 510080, China; [5]Qianyang Biomedical Research Institute, Guangzhou, Guangdong 510663, China; [6]Infectious Diseases Center, Guangzhou Eighth People's Hospital, Guangzhou Medical University, Guangzhou 510440, China; [7]Department of Medical Oncology, The Third Affiliated Hospital of Sun Yat-sen University, Guangzhou, Guangdong 510630, China; [8]Department of Pathology, The First Affiliated Hospital, Sun Yat-sen University, Guangzhou 510080, China

T cell lymphoma (TCL) is a highly heterogeneous group of diseases with a poor prognosis and low 5-year overall survival rate. The current therapeutic regimens have relatively low efficacy rates. Clinical studies of single-target chimeric antigen receptor T cell (CAR-T cell) therapy in T lymphocytes require large and multiple infusions, increasing the risks and cost of treatment; therefore, optimizing targeted therapy is a way to improve overall prognosis. Despite significant advances in bispecific CAR-T cell therapy to avoid antigen escape in treatment of B cell lymphoma, applying this strategy to TCL requires further investigation. Here, we constructed an alpaca nanobody (Nb) phage library and generated high-affinity and -specificity Nbs targeting CD30 and CD5, respectively. Based on multiple rounds of screening, bispecific NbCD30-CD5-CAR T cells were constructed, and their superior anti-tumor effect against TCL was validated *in vitro* and *in vivo*. Our findings demonstrated that Nb-derived bispecific CAR-T cells significantly improved anti-tumor efficacy in TCL treatment compared with single-target CAR-T cells and bispecific single chain variable fragment (scFv)-derived CAR-T cells. Because Nbs are smaller and less immunogenic, the synergistic effect of Nb-based bispecific CAR-T cells may improve their safety and efficacy in future clinical applications.

INTRODUCTION

T cell lymphoma (TCL), a heterogeneous lymphoma originating from mature T cells, exhibits various tumor localizations, pathological features, and clinical manifestations. TCL accounts for approximately 12% of non-Hodgkin's lymphoma cases and is categorized into cutaneous TCL and peripheral TCL (PTCL). PTCL is the predominant type and includes mesenchymal large cell lymphoma, angioblastoma, and peripheral non-specific TCL.[1] The age-adjusted incidence of TCL is fewer than 1/100,000 people, and fewer than 4,000 TCL cases are diagnosed annually in the United States.[2,3] Despite its low incidence, the majority of TCLs are characterized by an aggressive disease course and poor response to treatment. Most lymph node TCLs respond poorly to conventional chemotherapy regimens, especially in patients with disease progression after treatment, and the median overall survival is less than 1 year.[4–7] Despite tremendous advances in the treatment of hematologic malignancies, the disease is still not completely curable, and thus there is still potential to improve treatment outcomes. Currently, US Food and Drug Administration (FDA)-approved salvage therapies based on histone acetylation inhibitors only exhibit a 20%–25% efficacy rate. Monoclonal antibodies targeting cluster of differentiation (CD) 30 are more effective than small-molecule drugs but have a shorter remission duration.[8,9] Therefore, novel and optimized targeted therapies for patients with TCL are still worth exploring.[10]

Received 21 March 2023; accepted 25 July 2023;
https://doi.org/10.1016/j.omto.2023.07.007.

Correspondence: WenYu Li, Lymphoma Department, Guangdong Provincial People's Hospital, Guangdong Academy of Medical Sciences, Southern Medical University, Guangzhou 510080, China.
E-mail: lwy80411@163.com
Correspondence: Hui Zhang, Institute of Human Virology, Key Laboratory of Tropical Disease Control of the Ministry of Education, Guangdong Engineering Research Center for Antimicrobial Agent and Immunotechnology, Zhongshan School of Medicine, Sun Yat-sen University, Guangzhou, Guangdong 510080, China.
E-mail: zhangh92@mail.sysu.edu.cn
Correspondence: Bingfeng Liu, Institute of Human Virology, Key Laboratory of Tropical Disease Control of the Ministry of Education, Guangdong Engineering Research Center for Antimicrobial Agent and Immunotechnology, Zhongshan School of Medicine, Sun Yat-sen University, Guangzhou, Guangdong 510080, China.
E-mail: liubf5@mail.sysu.edu.cn

The chimeric antigen receptor (CAR), a receptor synthesized by genetic engineering, was proposed in the late 1980s by Gross et al.[11] It redirects antigen specificity to immune cells with high affinity in a major histocompatibility complex-independent manner. The most commonly modified cells are T cells, and the modified CAR-T cells are used to identify and eliminate cells expressing tumor-associated antigens (TAAs). When a specific TAA is recognized, CAR-T cells can activate a range of T cell effector responses, including cell proliferation, cytokine release, cellular metabolic alteration, and cytotoxicity, via phosphorylation activation signals.[12] Recently, CAR-T cell therapy has become an effective strategy for treating hematologic malignancies.[13]

CD19- or CD20-targeting CAR-T cell therapy is highly effective in patients with B-cell lymphoma, especially in those with refractory B cell lymphoma with poor prognosis after other therapies.[14,15] CAR-T cell therapy has also been used to treat TCL; however, this strategy faces challenges regarding whether the TAA targeted by CAR-T cells is also shared with normal T cells. Therefore, identifying the three types of cells (tumor T, normal T, and CAR-T cells) to prevent the fratricide of CAR-T cells may improve their *in vivo* expansion and persistence. Moreover, long-term T cell dysplasia caused by disruption of normal T cells puts patients at a serious risk of opportunistic infections.[16,17] Therefore, CAR-T cell therapy for T cell malignancies requires targeting of tumor T cells while retaining normal T cell or subpopulation functions. Most TAAs are expressed in normal and tumor cells, which makes design of the antigen recognition domain challenging.[18,19] Currently, strategies for targeting TCL while reducing CAR-T cell fratricide include utilizing pan-T antigens (such as CD5) that are downregulated during CAR-T cell expansion[20] or targeting TAAs expressed only in a portion of normal cell subgroups (such as CD4, CD30, or CCR4) to prevent non-specific cytotoxicity of CAR-T cells.[21–23] In preclinical study models, because CD5 antigens on cell membranes are internalized after ligand or antibody binding, CAR-T cells targeting CD5 can prevent their fratricide.[20,24] Additionally, CD30 is expressed in activated B and T cell subpopulations, including nearly all Hodgkin's lymphoma (HL), mesenchymal large cell lymphoma, and PTCL subpopulations; anti-CD30 CAR-T cells have also been evaluated in two phase I clinical trials, mainly in patients with HL.[22,23,25–27] In these studies, the number of B or T cells did not decline, and antiviral or anti-pathogen immunity remained unaffected.[22] These results are consistent with those observed in patients treated with brentuximab (an anti-CD30 monoclonal antibody).[28] In a clinical trial treating TCL,[22,27] the patient required injections of anti-CD30 CAR-T cells four times at the highest dose to achieve complete remission lasting 9 months. High-dose and multiple CAR-T cell administrations not only greatly increase the cost of treatment but also worsen the safety risk. Therefore, although CAR-T cell therapy against the single-target CD30 or CD5 in TCL has been proven to be feasible, its clinical efficacy needs further improvement.

Studies on B cell lymphoma have shown that CD19-negative clones emerge after CD19 single-target CAR-T cell administration because of tumor antigen escape, while these CD19-negative clones still maintain expression of other lymphoid-like antigens (such as CD20 and CD22) and even metastasize to bone marrow lineages.[29] This has led to development of combinatorial multitargeted immunotherapies, such as bispecific CAR-T cells, to reduce the possibility of immune escape and disease relapse.[30] A clinical trial using anti-CD19/anti-CD22 bispecific CAR-T cells successfully treated an adult patient with acute lymphoblastic leukemia (ALL) with no recurrence for more than 1 year after infusion.[31] Clinical studies of anti-CD19/anti-CD20 tandem CAR-T cells have also shown promising remission rates and long-term anti-tumor responses against refractory/relapsed B cell lymphoma.[32] In addition, anti-CD19/anti-CD123 bispecific CARs are more effective against B-ALL than single-target CAR.[30] Bispecific CAR-T cell therapy for B cell lymphoma treatment has progressed to not only avoid antigen escape but also generate synergistic effects. However, CAR designs for dual targets in the field of TCL treatment are still lacking.

Nanobodies (Nbs) are natural antibodies found in the peripheral blood of camelids. Nbs contain one heavy-chain variable region (V_H), lack light chains, and are half the molecular weight (12–15 kDa) of conventional human immunoglobulin G (IgG) antibodies.[33,34] Therefore, the small size, solubility, stability, and high antibody affinity of Nbs means that these multifunctional antibodies exhibit excellent properties and are widely used in anti-tumor therapy and diagnosis.[35–37] In recent years, Nbs have shown good potential for treating various tumors.[38] Nbs can reduce immunogenicity and increase the release of effector cytokines compared with scFv-derived CAR-T cells.[39–41] Further, bispecific Nb-derived CAR-T cells targeting CD13 and TIM3 have shown significant anti-tumor function and greatly reduced cytotoxicity in the treatment of acute myeloid leukemia.[42] There is already an FDA-approved CAR-T therapy, "cilta-cel," for multiple myeloma that uses an Nb-based design.[43] Here, we attempted to explore a bispecific Nb CAR-T cell that targets CD30 and CD5 to improve the efficacy against TCL.

RESULTS

Construction of a Nb immune library and screening of anti-CD30 and CD5 Nbs

Recent clinical studies have demonstrated the safety and efficacy of CD30- or CD5-targeted CAR-T cells in $CD4^+$ TCL treatment; however, current therapeutic regimens require a large number of modified cells and multiple infusions, which greatly increases the risk and cost of treatment.[22,27] Application of bispecific CAR-T therapy in B cell lymphoma has aided design and construction of bispecific CAR moieties for simultaneously targeting CD30 and CD5; the synergistic effect of these moieties in treatment of TCL needs to be verified.

Nbs have been widely developed because of their high binding affinity and low immunogenicity; however, this strategy has not yet been applied to TCL treatment. Therefore, we tried to develop Nbs specifically targeting CD30 and CD5 and construct an Nb-based bispecific CAR-T cells with stronger anti-tumor potency. To this end, we produced CD5 and CD30 antigens from transfected HEK293F cells. These antigens were then purified (Figure S1A) and subsequently

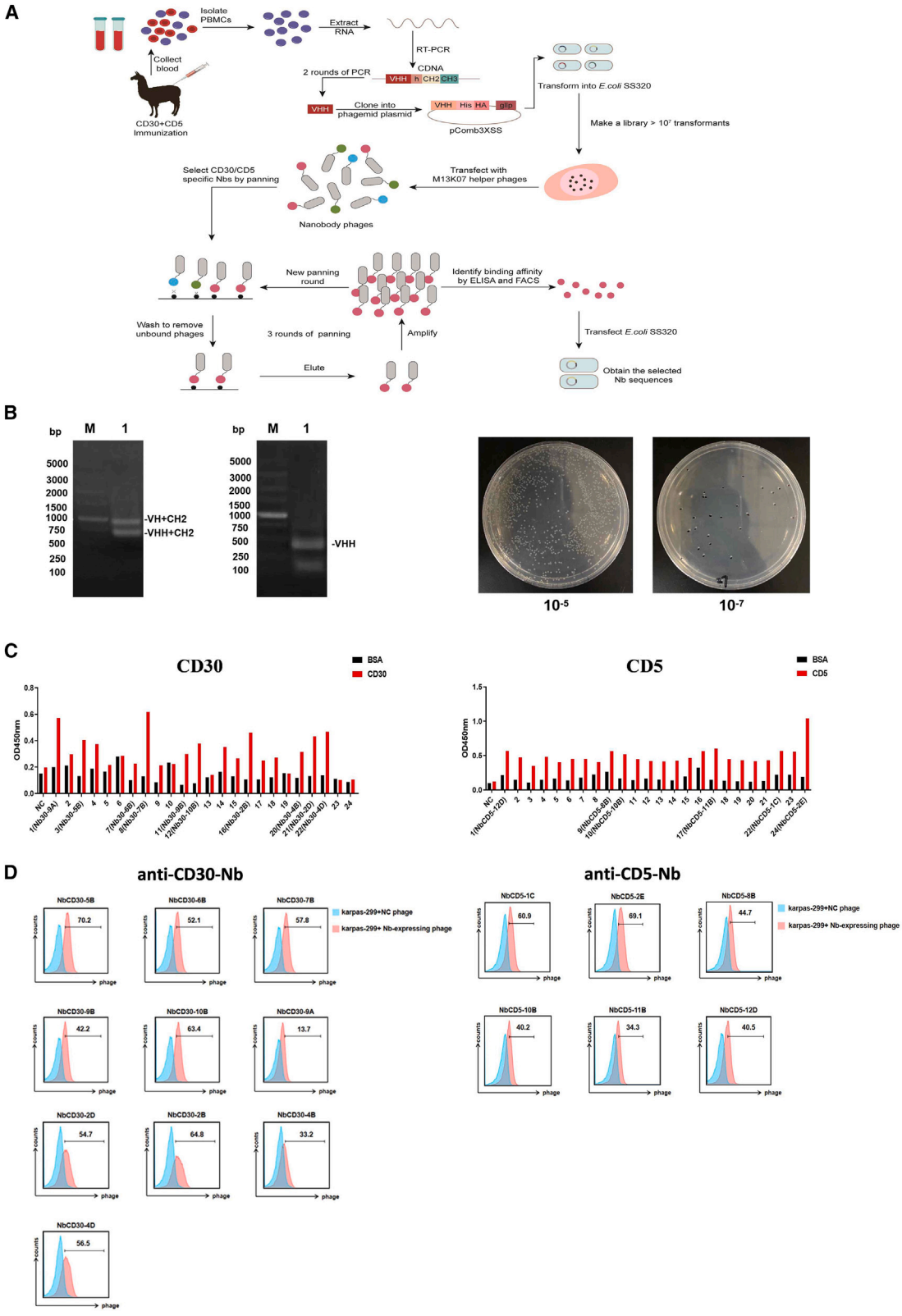

(legend on next page)

used to immunize alpacas four times. The antibody titer in the sera reached a 10^5 dilution compared with that in pre-immunized sera, which was sufficient for subsequent library construction (Figures 1A and S1B). Peripheral blood mononuclear cells were collected to construct the Nb phage library. This phage library had a 4.32×10^8 library volume and approximately 100% clonal positivity of insertion rate, meeting the requirements for Nb affinity screening (Figures 1A, 1B, and S2A). Monoclonal sequencing revealed that all variable regions of heavy-chain antibody inserts had genetically independent non-repeating amino acid sequences, which further demonstrated that the phage library had eligible sequence diversity (Figure S2B).

Subsequently, the phage library was used to screen for high-affinity Nbs against CD30 and CD5.[44–46] After three rounds of panning with purified CD30 or CD5 antigens, monoclonal clones were selected from the last panning phages, and their binding affinity to the corresponding antigens was verified using a phage enzyme linked immunosorbent assay (ELISA). The enrichment of phages with high affinity to antigens was significantly improved after three rounds of screening. Ten anti-CD30 phage clones and six anti-CD5 phage clones were obtained (Figure 1C). In addition, the identified phage clones were validated via target cell panning to avoid spatial site resistance. To this end, the monoclonal phages were incubated with targeting cells, and clones with high positive fluorescence were selected, including six CD30 clones (NbCD30-5B, NbCD30-6B, NbCD30-7B, NbCD30-10B, NbCD30-2B, and NbCD30-4D) and five anti-CD5 clones (NbCD5-1C NbCD5-2E, NbCD5-8B, NbCD5-10B, and NbCD5-12D) (Figure 1D).

In vitro binding affinity of the screened Nbs

The binding affinities of the selected monoclonal Nb sequences were evaluated. The sequences were connected to the human IgG Fc fragment in an eukaryotic expression vector (scFv-Fc served as positive control). The anti-CD30 scFv sequence was derived from the human monoclonal antibody brentuximab, and the anti-CD5 scFv sequence was derived from the human CD5-specific antibody H65.[47] The expressed Nb-Fc was purified, and its ability to bind target antigens was verified using ELISA; two Nbs targeting CD30 (5B and 2B) and two Nbs targeting CD5 (1C and 2E) were selected (Figures 2A and 2B). The results were consistent with the flow cytometry results, and the selected anti-CD30 or CD5 Nb-Fc had comparable or superior affinity to the target antigen, in contrast with the corresponding scFv-Fc (H65 or brentuximab) (Figure 2C).

An obvious cross-reaction between anti-CD30 scFv (brentuximab) and CD5 was observed using ELISA; however, the selected NbCD30-Fc had no significant cross-reactivity with CD5, and NbCD5-Fc did not cross-react with CD30 (Figure 2C). These results further validated the superior specificity and lower off-target risk of the selected Nbs. Therefore, we successfully constructed an Nb phage library and obtained several Nbs capable of targeting CD30 and CD5 with high affinity and specificity.

Construction of Nb-derived CAR-T cells

Optimal CAR moieties for use in further experiments were identified. $CD8^+$ T lymphocytes transduced with lentiviral vectors encoding the selected Nb-CAR moieties were mixed with target cells expressing CD5 and CD30 (Figure 2D). The two Nb-derived CARs against CD5 and NbCD5-1C-CAR-T cells reached 75% specific cytotoxicity at a 10:1 effector cell-to-target cell (E:T) ratio, while NbCD5-2E-CAR-T cells showed a minimal difference compared with the control group. In contrast, the two Nb-derived CARs against CD30, NbCD30-5B-CAR-T and NbCD30-2B-CAR-T, exhibited significant cytotoxicity against target cells at a 10:1 E:T ratio (67% and 63%, respectively). NbCD30-5B was less efficient than NbCD30-2B at lower E:T ratios (Figure 2D). Therefore, NbCD5-1C and NbCD30-2B were selected as the final Nb candidates.

The molecular docking of the antigens and antibodies predicted theoretical binding models of either CD30 or CD5 to their corresponding Nbs. NbCD30-Fc and NbCD5-Fc had lower ΔG free energies than scFv-Fc, suggesting that the Nbs may bind more tightly to the antigens (Figure 3A). Surface plasmon resonance was performed using a BIAcore system to determine the binding affinity between the Nbs and antigens. Purified CD30 or CD5 was immobilized on a CM5 sensor chip (carboxymethylated dextran covalently attached to a gold surface). The surface plasmon resonance sensorgrams also confirmed that all four Nbs had a very strong affinity for their corresponding antigens. The K_D values of NbCD5-1C-Fc and CD5-scFv-Fc to the CD5 antigen were 6.30×10^{-11} and 1.17×10^{-10} M, respectively, and the Nbs showed a higher affinity than scFv. In contrast, the K_D value of NbCD30-2B-Fc to the CD30 antigen (4.17×10^{-11} M) was lower than that of CD30-scFv-Fc (0.96×10^{-11} M) (Figure 3B). The CD30-scFv antibody showed a potential off-target property according to the ELISA results, whereas NbCD30-2B-Fc Nb did not cross-react with CD5 and showed better specificity (Figure 2C). Therefore, both Nbs screened using alpaca immunization exhibited comparable or higher efficiency than scFv.

Nb-derived bispecific CD30-CD5-CAR-T cells enhance anti-tumor capacity *in vitro*

A bispecific Nb by tandem linkage of NbCD5-1C and NbCD30-2B with Fc was constructed and purified to test its affinity using

Figure 1. Construction of the Nb phage library and screening of anti-CD30 Nbs and anti-CD5 Nbs

(A) Schematic of construction of the Nb phage library and screening of Nbs. (B) The variable domain of heavy chain of heavy-chain antibody (VHH) genes were obtained by two-step PCR, and the library size was measured by counting the colonies after serial dilution (M, DNA marker; 1, PCR product). (C) Monoclonal phage ELISA. 24 positive phages from the three rounds of panning were tested for binding affinity by ELISA with CD30- and CD5-coated plates. (D) Flow cytometry screening of monoclonal phages capable of binding to cells. Karpas-299 cells were used as target cells to validate positive monoclonal phages by flow cytometry. Negative control (NC) phages that did not express Nbs were used as a negative control.

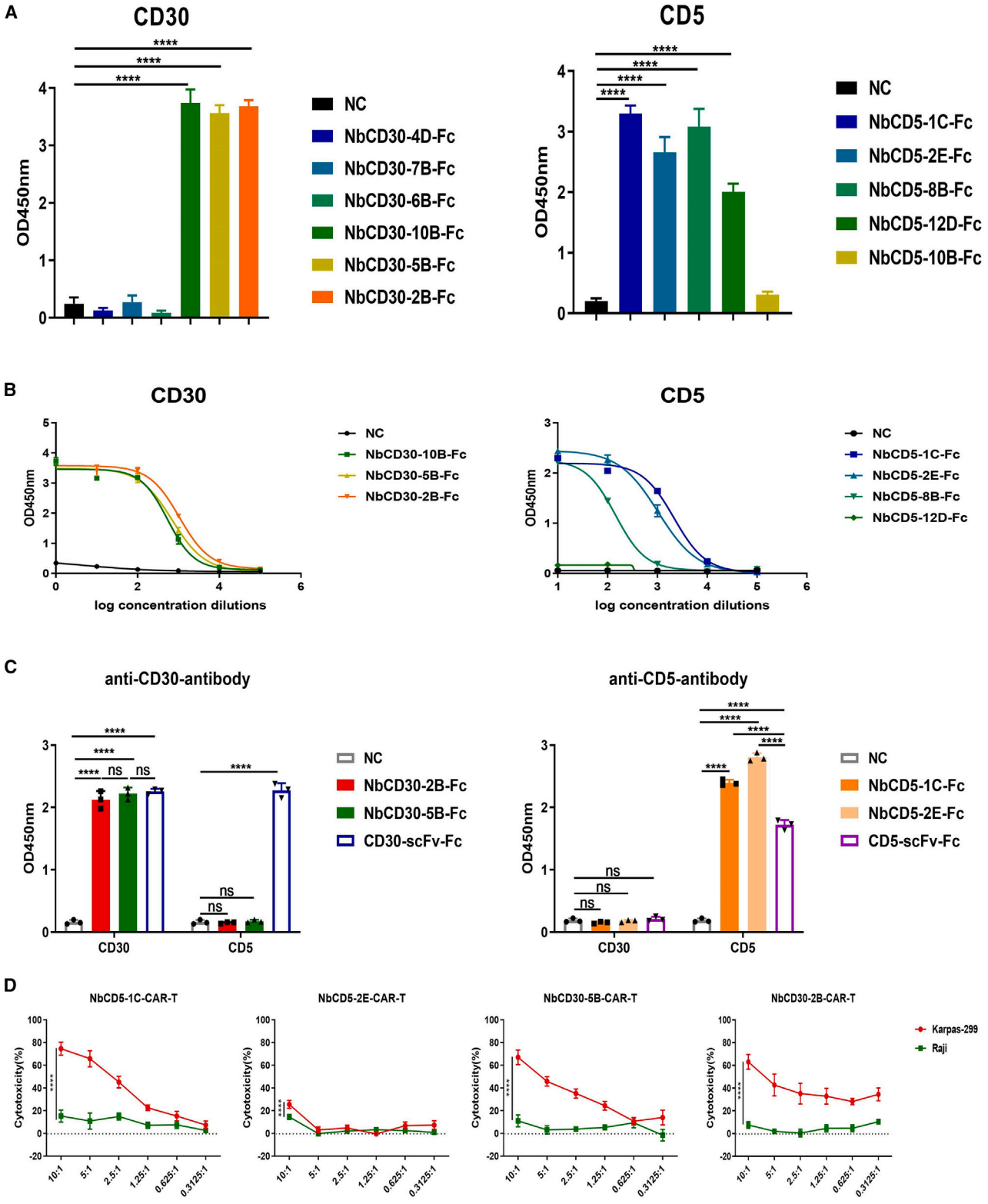

(legend on next page)

ELISA. The bispecific NbCD30-CD5-Fc strongly bound to CD30 and CD5 antigens, and there was no difference in its affinity compared with that of single-specific Nb-Fc binding to the corresponding targets (Figure S3).

The binding affinities of the Nbs to corresponding antigens and function of the derived single-targeted CAR-T cells were verified (Figure 2D). Next, to further verify the synergistic effect of bispecific moieties in the treatment of TCL, we used tandem connection of two different Nbs to design the bispecific-target CAR-T cells according to previous studies.[48,49] A single or bispecific Nb-CAR designed using tandem linkage of NbCD5-1C and NbCD30-2B with a $(GGGGS)_4$ flexible peptide as the connecting sequence was constructed. scFv-derived bispecific CD30-CD5-CAR-T cells were also constructed to verify their enhanced efficacy. The intracellular domains of CAR molecules were determined based on previous publications.[50,51] The scFv or Nb sequence was followed by the human CD8a transmembrane and intracellular domains, which included human CD28 (nucleotides 460–660; GenBank: NM_006139.3), CD137(nucleotides 640–765; GenBank: NM_001561.5), and CD3ζ (nucleotides 160–492; GenBank: NM_198053.2) in tandem with GGGGS sequences inserted between each signaling domain. The CAR moiety was inserted into a lentiviral vector (Figures 4A and 4B).[50] CAR expression was evaluated via western blotting (Figures S4A and S4B). CAR-T cells were prepared after packaging the lentivirus, and the infection rate was determined to be approximately 20% after 48 h using flow cytometry (Figure S5). One of the advantages of bispecific CAR-T cells is their ability to prevent antigen escape and reduce off-target effects. To identify the function of single- or bispecific CARs for use in further experiments, $CD8^+$ T lymphocytes transduced with lentiviral vectors encoding the above-mentioned CAR moieties were mixed with Karpas-299 ($CD30^+$ $CD5^+$) or aji ($CD30^-$ $CD5^-$) cells for *in vitro* killing assays. The cytotoxicity of single-target anti-CD5 scFv-CAR-T cells or anti-CD30 scFv-CAR-T cells to Karpas-299 cells at a 10:1 E:T ratio was approximately 44% and 42%, respectively, whereas the cytotoxicity mediated by bispecific CAR-T cells was approximately 56%, which was more effective than single-target anti-CD30 or anti-CD5 scFv-CAR-T cells (Figure 4C). The single-target Nb-CAR-T cells and bispecific NbCD30-CD5-CAR-T cells displayed potent cytotoxic activity toward Karpas-299 cells ($CD30^+$ $CD5^+$) at the indicated E:T ratios *in vitro* (Figure 4D). The cytotoxicity of bispecific NbCD30-CD5-CAR-T cells to Karpas-299 cells at a 5:1 or 2.5:1 E:T ratio was more effective than that of single-target anti-CD30 CAR-T cells (5:1 ratio, $p < 0.001$; 2.5:1 ratio, $p < 0.001$) or anti-CD5 CAR-T cells (5:1 ratio, $p < 0.01$; 2.5:1 ratio, $p < 0.0001$) (Figure 4D). To exclude the possibility of background lysis mediated by $CD8^+$ T cells with a non-functional CAR moiety, CD19-CAR as a negative control was used in *in vitro* CAR-T cell assays (Figure S6). The results demonstrate that CD19-CAR-T cells do not exhibit specific targeting toward $CD19^-$ Karpas-299 cells. Moreover, the cytotoxicity of bispecific Nb-CAR-T cells to Karpas-299 cells was also more effective than that of bispecific scFv-CAR-T cells (65% specific cytotoxicity for the Nb-CAR-T cell group versus 47% for the scFv-CAR-T cell group at a 5:1 ratio and 61% versus 42% at a 2.5:1 ratio, respectively; Figure 4E). Moreover, the specificity of the antigen recognition domains was verified using SupT1 cells expressing high levels of CD30 and very low levels of CD5 to test their cytotoxic specificity. Single- or bispecific CAR-T cells were co-cultured with SupT1 cells, and the results showed that anti-CD5 scFv-CAR-T cells displayed minimal cytotoxic activity against SupT1 ($CD30^+$ $CD5^-$) cells, whereas single-specific anti-CD30 scFv-CAR-T cells or bispecific anti-CD30-CD5 scFv-CAR-T cells exhibited potent cytotoxicity (40%) at a 2.5:1 E:T ratio (Figure 4C). For Nb-CAR-T cells, single-targeted NbCD5-CAR-T cells did not exhibit cytotoxic effects, whereas bispecific NbCD30-CD5-CAR-T cells still exhibited strong cytotoxic effects compared with the NbCD5-CAR-T group ($p < 0.0001$) and achieved a killing rate of nearly 50% at a 5:1 E:T ratio (Figure 4D). We also generated $CD5^+$ Raji cells by overexpressing the CD5 antigen on $CD30^-CD5^-$ Raji cells to serve as a control in the cytotoxicity assay of CAR-T cells (Figure S7). The results demonstrated that NbCD30-CD5-CAR-T cells and NbCD5-CAR-T cells exhibited specific targeting toward $CD5^+CD30^-$ target cells ($CD5^+$ Raji cells), whereas NbCD30-CAR-T cells showed no cytotoxic effect. Moreover, the specificity was confirmed by the absence of cytotoxicity of bispecific scFv or Nb-CAR-T cells after co-culture with Raji cells ($CD30^-$ $CD5^-$) (Figure 4E). Therefore, bispecific Nb CAR-T cells have a specific cytotoxic function and can effectively enhance targeting potency.

The *in vitro* cytokine (interferon γ [IFN-γ], tumor necrosis factor alpha [TNF-α], interleukin-2 [IL-2], and granzyme B) secretion function of single- and bispecific Nb CAR-T cells was measured after co-culture with target cells (Figure 4F). Secretion of effector cytokines, including IFN-γ, TNF-α, IL-2, and granzyme B, in the supernatants of single- and bispecific target CAR-T cells was significantly higher than in the mock group after co-culturing with $CD30^+$ $CD5^+$ Karpas-299 cells (Figure 4F). The levels of these cytokines secreted by bispecific NbCD30-CD5-CAR-T cells were significantly higher than those secreted by single-target Nb CAR-T cells (Figure 4F). In addition, the function specificity was confirmed by the absence of cytokine secretion after co-culture with $CD30^-$ $CD5^-$ Raji cells (Figure 4F). Secretion of IFN-γ was further examined using an enzyme-linked

Figure 2. *In vitro* binding ability validation of the screened Nbs

(A) The biding affinity of Nb-Fc to CD30 or CD5 was measured by ELISA. (B) Three anti-CD30 Nbs and four anti-CD5 Nbs were selected, and we performed ELISA at the indicated dilution ratios by incubation with the corresponding antigens. Fc served as negative control. (C) Detection of the binding affinity of the Nb-Fc or scFv-Fc antibodies to CD5 or CD30, respectively, by ELISA. (D) Single-target NbCD30 or NbCD5-CAR-T cells were co-cultured with Karpas-299 cells ($CD30^+$ $CD5^+$) at different effector-to-target ratios for 24 h, and the specific cytotoxicity was determined by Lactic Dehydrogenase (LDH) assay. ****$p < 0.0001$ for one-way ANOVA with multiple-comparisons test. All data are mean ± standard error.

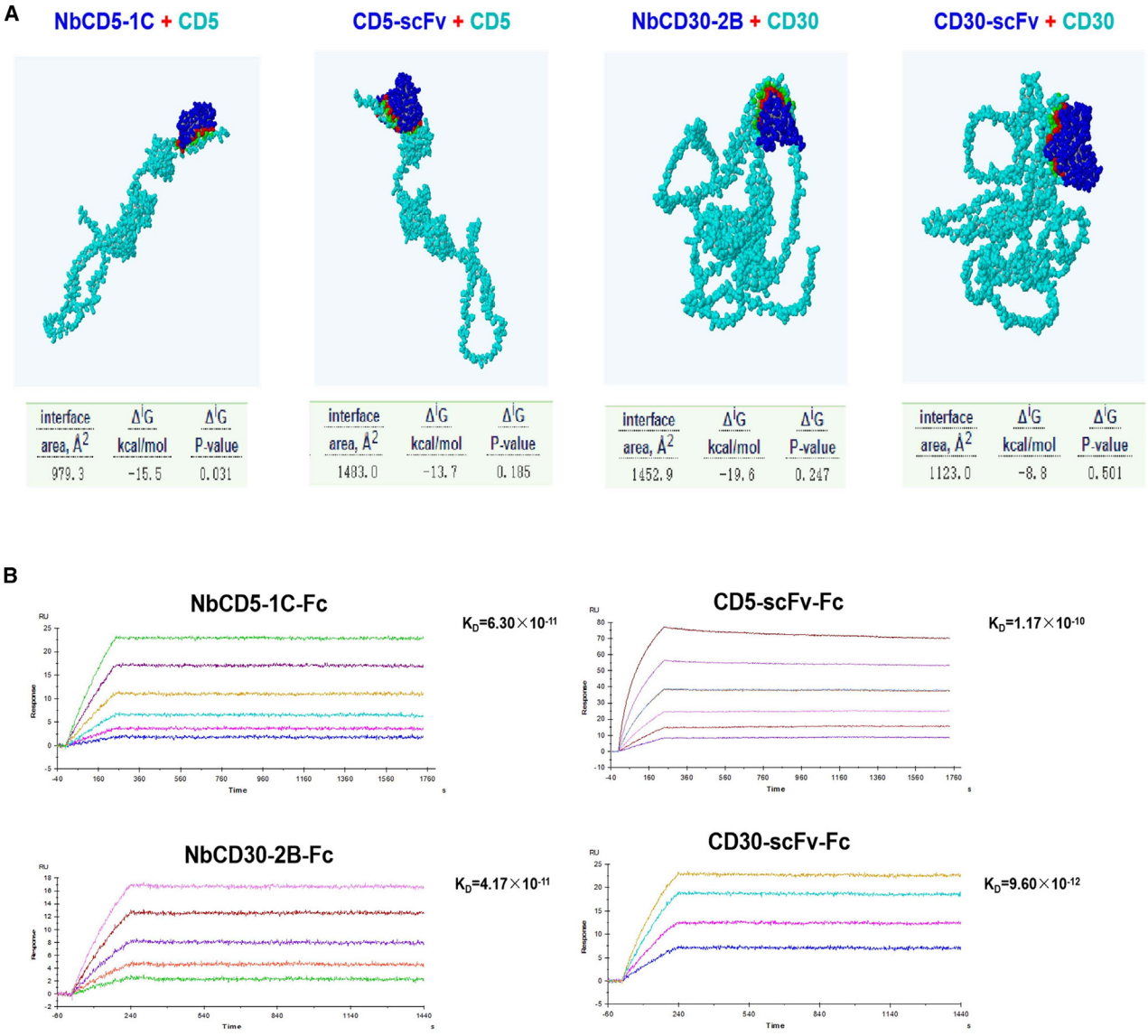

Figure 3. The binding ability was predicted by molecular docking and verified by SPR experiments

(A) Molecular docking prediction model of anti-CD30/CD5 Nbs or scFv to corresponding antigens. The light blue structure indicates the antigen, the dark blue structure indicates the antibody, the interface area (red) indicates the region of the two proteins in contact with each other, and ΔG indicates the free energy of binding. (B) SPR experiments were performed to measure the binding affinity of Nb-Fc or scFv-Fc on its corresponding antigen.

immunosorbent spot assay; IFN-γ secretion by bispecific Nb CAR-T cells was significantly higher than that of the single-target Nb CAR-T group (Figure 4G). Therefore, the functional potency of bispecific Nb-CAR-T cells was further validated by secretion of various cytokines.

Nb-derived CD30 and CD5 bispecific CAR-T cells enhanced anti-tumor potency *in vivo*

Bispecific anti-CD30-CD5-CAR-T cell function was further validated by transferring CAR-T cells into Karpas-299 tumor-bearing immunodeficient mice and examining their efficacy against tumor growth (Figures 5A, 5B, and S8A). The tumor size was significantly inhibited in the single-target CAR-T cell groups compared with the control group, and tumor suppression by bispecific anti-CD30-CD5-CAR-T cells was significantly improved compared with single-target CD30-CAR-T cells (Figures 5A–5C). These results suggest that the enhanced anti-tumor activity of anti-CD30-CD5-CAR-T cells *in vivo* may be due to the optimal binding affinity of anti-CD30 and anti-CD5 scFv/Nbs to target antigens and avoidance of tumor cell immune escape. Therefore, our Nb-derived CAR-T cells have a superior capability to suppress TCL growth *in vivo*, and bispecific NbCD30-CD5-CAR-T cells further enhance anti-tumor potency.

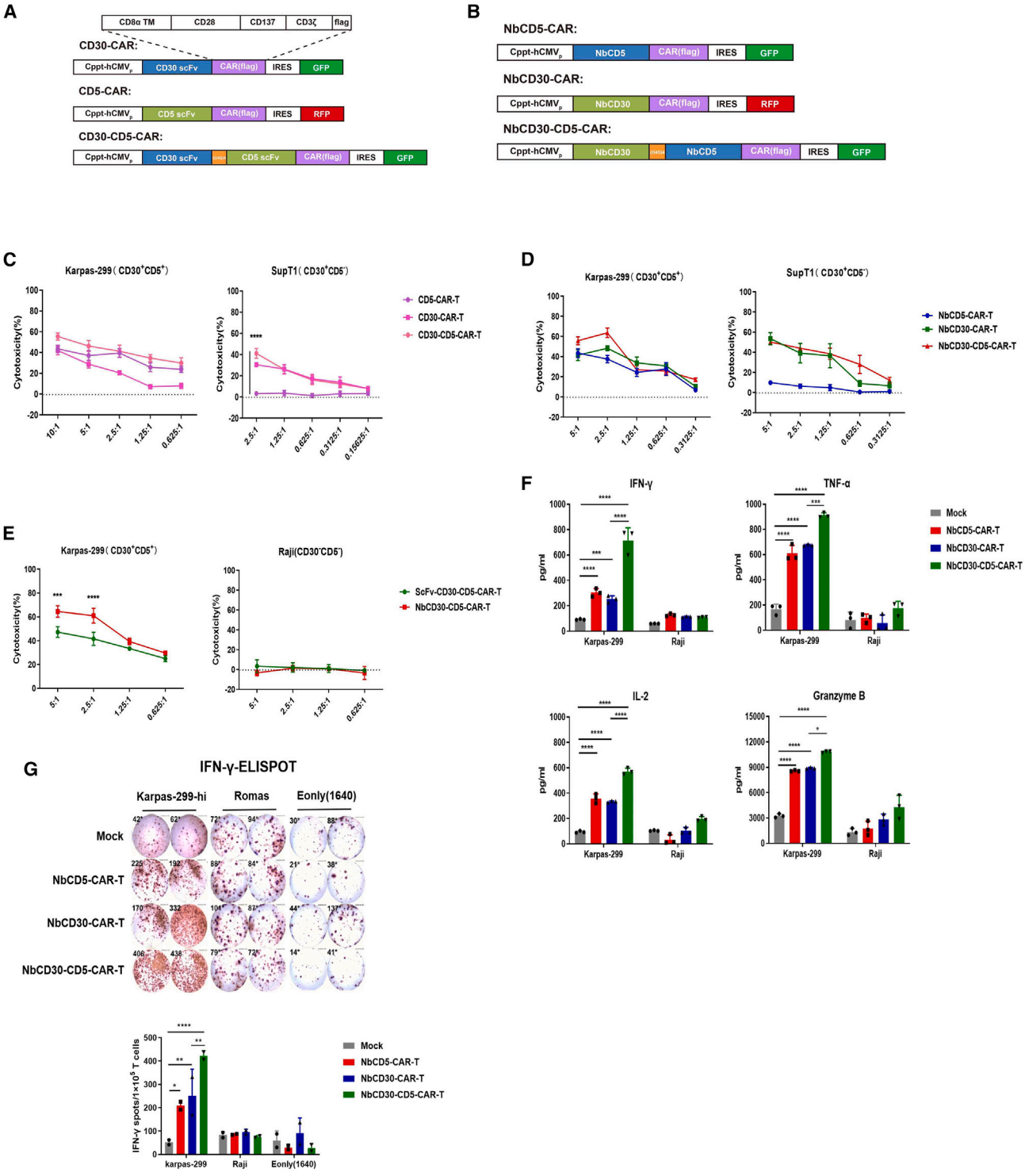

Figure 4. Construction of bispecific Nb/scFv-derived CAR-T cells to verify *in vitro* function

(A) Schematic of CAR structure and single- or bispecific scFv-CAR. (B) Schematic of single NbCD30/NbCD5-CAR or bispecific NbCD30-CD5-CAR. (C) Single-or bispecific scFv-CAR-T cells were co-cultured with Karpas-299 cells ($CD30^+$ $CD5^+$) or SupT1 cells ($CD30^+$ $CD5^-$) at the indicated E:T ratios for 24 h, and the specific cytotoxicity was determined by LDH assay. The data shown are representative results of three independent replication experiments. (D) Single-or bispecific Nb-CAR-T cells were co-cultured with Karpas-299 cells ($CD30^+$ $CD5^+$) or SupT1 cells ($CD30^+$ $CD5^-$) at different E:T ratios for 24 h, and the specific cytotoxicity was determined by LDH assay. The data shown

(legend continued on next page)

Next, the infiltration ability of anti-CD30-CD5-CAR-T cells was assessed in subcutaneous tumor tissues of the experimental mice by flow cytometry and immunofluorescence assays. Flow cytometry revealed that tumor-infiltrating T cells of the single- and bispecific Nb CAR-T cell groups were significantly increased compared with the mock group, and the infiltrating Nb CAR-T cells secreted higher levels of effector cytokines, such as IFN-γ, IL-2, and granzyme B (Figure 6A). Notably, the levels of IL-2 and granzyme B secreted by bispecific NbCD30-CD5-CAR-T cells were significantly higher than those of single-target Nb CAR-T cells (Figure 6A). The immunofluorescence results of tumor tissue sections also showed that the ratio and number of tumor-infiltrating T cells in the single- and bispecific Nb-CAR-T cell groups increased significantly compared with those in the mock group. Consistent with the flow cytometry results, infiltrating T cells in the NbCD30-CAR-T and NbCD30-CD5-CAR-T cell groups secreted higher levels of IFN-γ and granzyme B cytokines than those in the mock group (Figure 6B). Bispecific scFv-CAR-T cells also exhibited enhanced *in vivo* anti-tumor potency compared with single-targeted scFv-CAR-T cells (Figures S8B, S8C, S9A, and S9B).

The *in vivo* therapeutic effect of Nb-CAR-T cells was evaluated against TCL by monitoring the survival of tumor-bearing mice. All mice in the mock group died 45 days after tumor cell transplantation, while mice treated with single-target NbCD30 or NbCD5-CAR-T cells had a longer lifespan. Notably, bispecific NbCD30-CD5-CAR-T cells further increased the lifespan of tumor-bearing mice by up to 90 days compared with the single-target Nb-CAR-T group (Figure 6C). These results demonstrate that single- and bispecific Nb-CAR-T cells can recognize and effectively eliminate TCL *in vitro* and *in vivo* and that bispecific Nb-CAR-T cells further increase anti-tumor potency to prolong the lifespan. Furthermore, NbCD30-CD5-CAR-T cells did not induce any potential toxicity in mice (Figure S10). There was no off-target damage to normal tissue, indicating that the treatment is safe. Therefore, Nb-derived CD30 and CD5 bispecific CAR-T cells enhanced anti-tumor potency *in vivo*. Moreover, the synergistic effect of the bispecific CAR-T cell strategy for TCL treatment was validated.

DISCUSSION

In this study, we successfully identified and optimized Nbs against CD5 and CD30 with superior affinity and specificity. We constructed Nb-based CAR-T cells and evaluated their efficiency in treating TCL using a series of *in vitro* and *in vivo* experiments. The superior affinity and specificity of Nbs were confirmed, and the synergistic anti-tumor efficacy of Nb-derived bispecific CAR-T cells for treatment of TCL was verified. TCL is a group of heterogeneous lymphomas caused by mature T cells with a low incidence.[2,3] However, the overall 5-year survival rate is low because of its aggressive progression, leading to poor treatment response and prognosis. In the past 10 years, the FDA has approved pralatrexate,[52] romidepsin,[53] bentuximab vedotin,[54] and belinostat[55] for treatment of patients with relapsed/refractory lymphoid node TCL. Although these drugs improve the selection of treatment regimens, drug response rates are typically lower than 30%, and the duration of response is limited. Novel targeted therapeutic strategies for patients with TCL have been widely explored, including histone deacetylase inhibitors, monoclonal antibodies, CAR-T cells, phosphatidylinositol 3-kinase inhibitors, and mesenchymal lymphoma kinase inhibitors.[10] These targeted therapies have prolonged the lifespan of patients with TCL. However, the clinical results are still unsatisfactory, and the disease remains incurable.

Recently, with development of immunotherapies, genetically modified CAR-T cells have become an effective treatment strategy for hematologic malignancies,[13] especially in patients with refractory B cell lymphoma and poor prognosis after traditional treatment.[14,15,56,57] However, because of the antigen escape of cancer cells, some patients become insensitive to CD19-CAR-T cell treatment. To address this issue, novel therapeutic targets (such as CD20, CD22, and CD123) have been identified, and combination therapy, including bispecific CARs, has been developed to prevent tumor recurrence.[58–60] Furthermore, bispecific CAR-T cells targeting CD19/CD22, CD19/CD20, and CD19/CD123 have led to tremendous progress in B cell lymphoma treatment.[30–32]

Bispecific CAR-T cells can not only avoid antigen escape but also exhibit synergistic effects that significantly improve anti-tumor efficacy. However, this novel strategy is less developed for treatment of TCL. Preclinical data have shown that single-targeted anti-CD4-CAR-T cells are effective in eradicating lymphoma cells.[21] However, they may also induce CD4 T cell dysplasia, which may lead to an HIV/AIDS-like syndrome. In preclinical studies of CD5-targeting CAR-T cells, the CD5 antigen is internalized after binding to its ligands or antibodies, leading to a decrease in its own expression.[20,24] Although CAR-T cells targeting CD30 have been shown to be safe and effective for clinical use, this regimen requires multiple injections at a high dose.[22,27] Other CAR-T cell designs, including those targeting CD7 or CCR4, have shown encouraging progress. However, these single-target therapies against TCL still have the problems of fratricide and lower efficiency.[61–63] In the current study, bispecific CAR-T cells targeting CD30 and CD5 largely improved the efficacy and specificity against TCL.

Tumor membrane proteins, such as specific glycoproteins, can be recognized as TAAs, and most extracellular segments of CARs are scFv structures, which may have problems such as insufficient stability, potential aggregation, cross-reaction, and difficulty of mass

are representative results of three independent replication experiments. (E) Bispecific Nb-CAR-T and scFv-CAR-T cells were co-cultured with Karpas-299 cells ($CD30^+$ $CD5^+$) or Raji cells ($CD30^-$ $CD5^-$) at different E:T ratios for 24 h, and the specific cytotoxicity was determined by LDH assay. (F) NbCD30/CD5-CAR-T cells or mock T cells (untransduced T cells) were incubated with tumor target cells (Karpas-299) for 24 h. The levels of IFN-γ, TNF-α, IL-2, and granzyme B in culture supernatants were measured by ELISA. (G) CAR-T cells or control T cells were incubated with tumor target cells (Karpas-299) at a 1:1 ratio for 24 h. Secretion of IFN-γ was measured by ELISpot assay. All data are representative of three independent replication experiments. All data are mean ± standard error; *$p < 0.05$, **$p < 0.01$, ***$p < 0.001$, ****$p < 0.0001$ for one-way ANOVA.

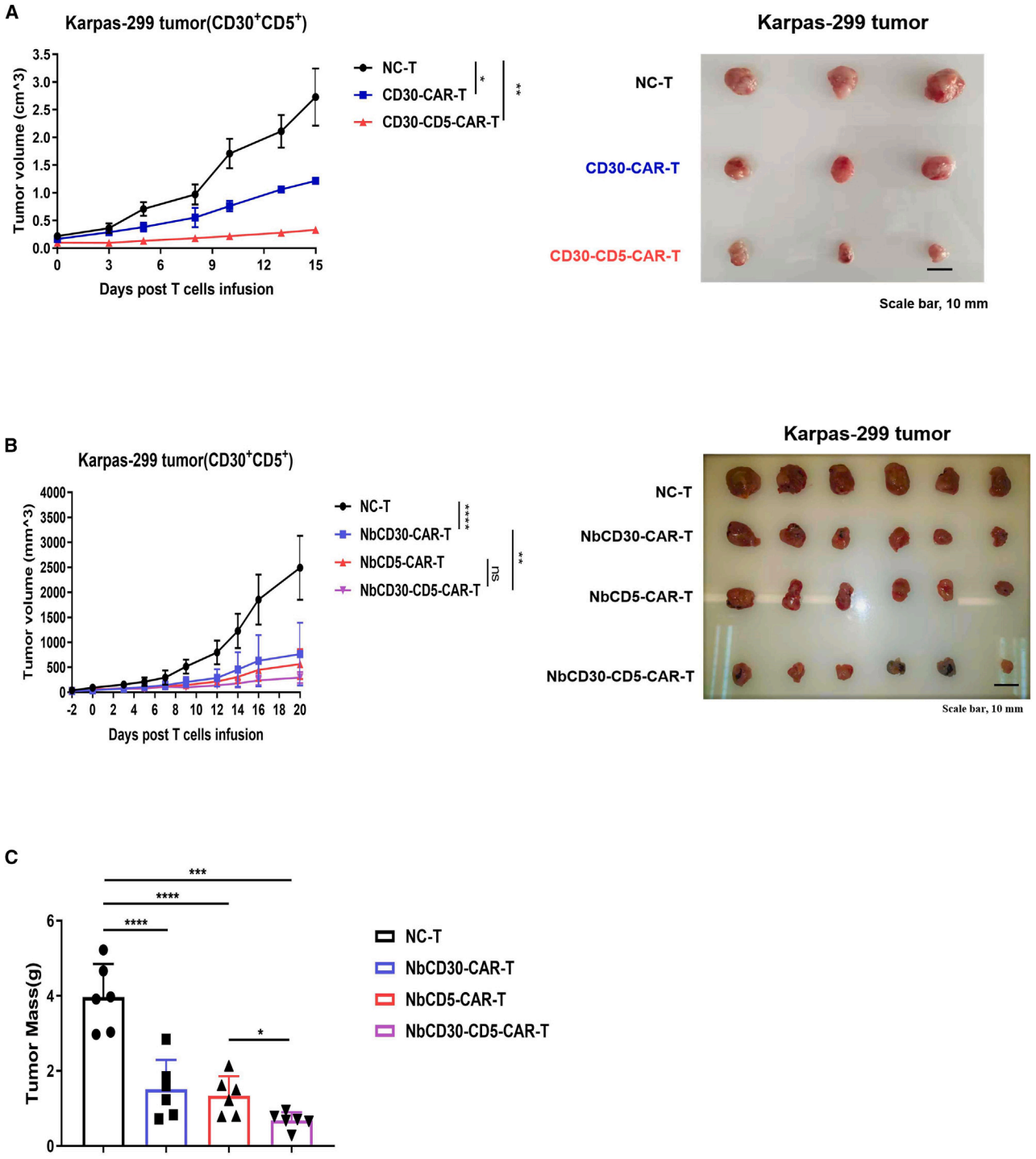

Figure 5. Bispecific CD30-CD5-CAR-T cells are more effective for tumor growth suppression

(A and B) 6×10^6 Karpas-299 cells were inoculated subcutaneously into NCG mice. The tumor reached 100 mm^3 after 7–10 days. Various T cells were infused via tail vein injection. Tumor engraftment was monitored every 2–3 days (1–2 μg of human IL-2 per mouse was injected at a frequency of 2–3 days). s.c., subcutaneous; i.v., intravenous; i.p., intraperitoneal. Tumor volumes were monitored after injection of CAR-T cells (scale bar, 10 mm). (C) The tumor mass was quantified. All data are mean ± standard error; *p < 0.05, **p < 0.01, ***p < 0.001, ****p < 0.0001 for one-way ANOVA.

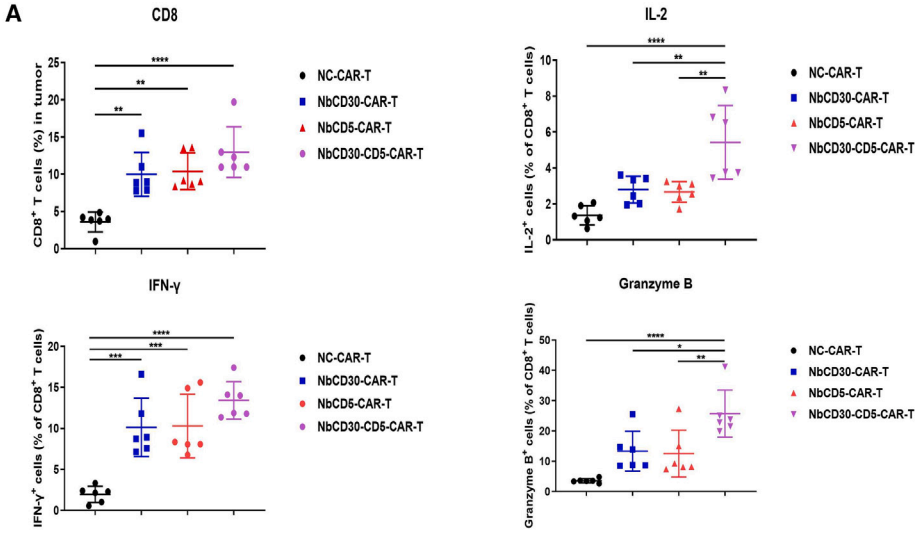

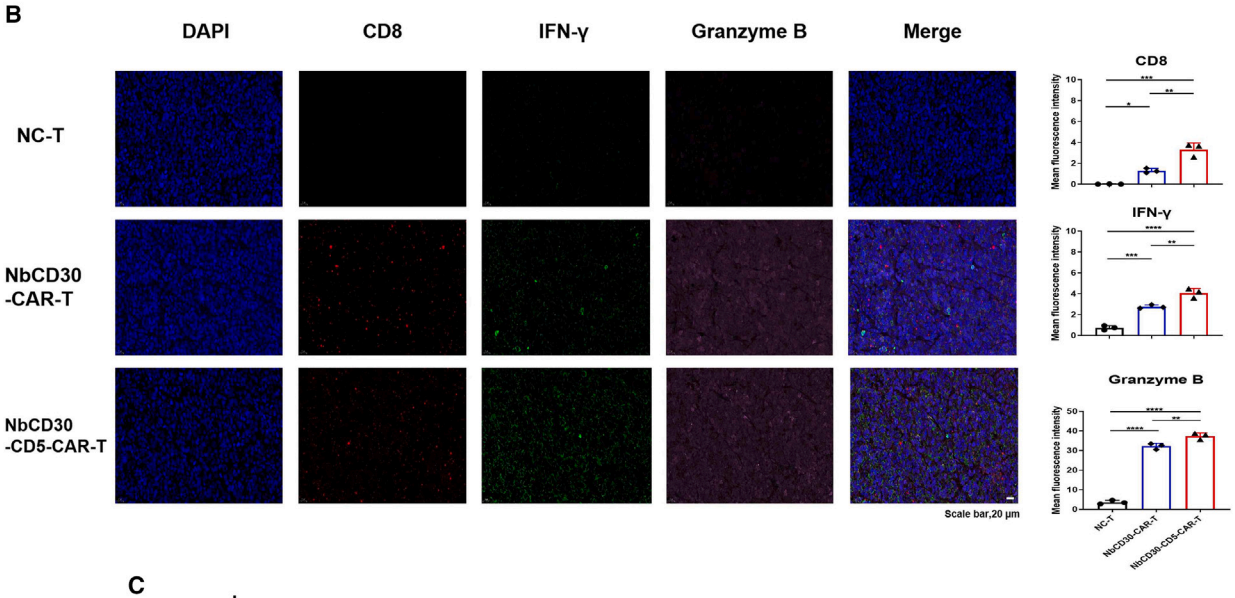

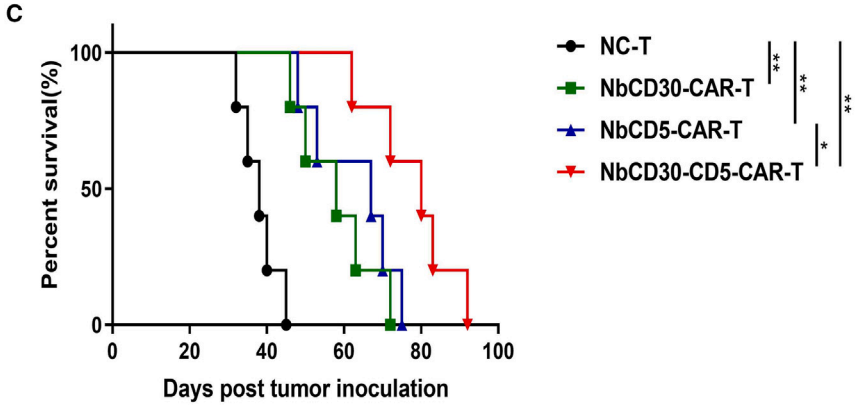

(legend on next page)

production.[64] Therefore, identification of more efficient antibodies is urgently needed, and the newly developed Nb technology appears to be a suitable solution. Nbs are the smallest known functional antigen recognition fragments (12–15 kDa)[37] compared with monoclonal antibodies (approximately 150 kDa) and antigen-binding fragments (approximately 55 kDa). Nbs are small but stable, can retain 80% activity at 37°C for a week, and restore their natural conformation after denaturation at 90°C.[65,66] Furthermore, although Nbs lack a light chain, they have superior specificity, high affinity, and low immunogenicity.[40] CAR-T cells based on Nb constructs have already been developed. Nb CAR-T cells targeting fibronectin's alternatively spliced EDb (EIIIB) impair tumor neovascularization, reduce the blood supply to the tumor, and make it more permeable to oncology drugs.[67] CD105- or CD72-targeting Nb-CAR-T cells have also demonstrated powerful anti-tumor capabilities.[68,69] Clinical studies have shown that Nb-derived CAR-T cells against CD7 have durable anti-tumor responses in patients with relapsed and refractory T cell ALL/acute lymphoblastic lymphoma.[70] Therefore, Nb-based CAR-T cell therapy may be a promising strategy for tumor treatment.

The current study demonstrates the enhanced synergistic effect of bispecific anti-CD30-CD5-CAR-T cells against TCL. Given the issues of scFv specificity and immunogenicity, CD30 and CD5 antigen proteins were purified to immunize alpacas and generate an Nb phage library; the specific Nbs were screened and optimized against CD30 or CD5 antigens. The selected Nbs were demonstrated to have higher affinity and specificity than scFv. We constructed bispecific Nb-CD30-CD5-CAR-T cells that further enhanced the *in vitro* and *in vivo* efficacy against TCL. Nbs are smaller and less immunogenic; therefore, the synergistic effect of Nb-based bispecific CAR-T cells may improve the safety and effectiveness of TCL treatment in clinical practice.

Nb-based bispecific CAR-T cells have shown encouraging results *in vitro* and in tumor-bearing mice. This strategy could be further evaluated by constructing xenograft mouse tumor models derived from TCL samples. If the results also show significant advantages compared with previous studies, clinical trials will be performed with the aim of achieving better outcomes in patients with TCL. It is expected that, with development of more powerful and durable CAR-T cell therapies to re-build anti-tumor immunosurveillance, long-term remission and survival of patients with TCL may be achieved.

MATERIALS AND METHODS

Cell lines

HEK293T cell lines were obtained from the ATCC and cultured in Dulbecco's modified Eagle's medium (Gibco, Invitrogen, Carlsbad, CA, USA) supplemented with 10% fetal bovine serum (FBS) (Gibco, Invitrogen). Karpas-299 cell lines were donated by the Lymphoma Department of Guangdong Provincial People's Hospital. Raji, Jurkat, and SupT1 cells were also obtained from the ATCC. Karpas-299, Raji, Jurkat, and SupT1 cells were cultured in RPMI 1640 medium (Gibco, Invitrogen) supplemented with 10% FBS (Gibco, Invitrogen). HEK293F cells were also obtained from the ATCC and cultured in Union-293 cell culture medium (Union Biotech [Shanghai]). All cell culture media contained 100 U/mL penicillin and 100 μg/mL streptomycin. Cells were maintained in a humidified atmosphere containing 5% CO_2 at 37°C.

Construction of the CAR lentiviral vector

The intracellular structural domain of the CAR molecule in the lentiviral vector used in this study follows previous publications from our laboratory.[50,51] The anti-CD30 scFv sequence was derived from brentuximab, and the anti-CD5 scFv sequence was derived from the humanized H65 antibody,[47] then the single- or bispecific scFv was linked to the CAR structure constructed in our laboratory, respectively, the scFv followed by CD8a transmembrane domain and intracellular domains, which contain CD28, CD137, and CD3ζ in tandem with GGGGS sequences inserted between each domain. The NbCD30, NbCD5, or NbCD30-CD5 sequence was ligated to the CAR structure constructed in our laboratory to form the Nb-derived CARs. The CAR moiety was inserted into the lentiviral vector pCPPT-IRES (Internal Ribosome Entry Site) -GFP/RFP (Red Fluorescent Protein). Cells infected by pseudotyped lentiviruses can be detected by fluorescence.

Western blot

Expression of the CAR was detected by western blot assay after transfection of lentiviral vector to HEK293T cells. The lentiviral CAR plasmid was transfected into HEK293T cells with the liposome transfection reagent lipo2000, and the cells were collected and lysed after 48 h. The expression of chimeric antibody protein-CAR was detected by an anti-FLAG antibody (MBL, M185-3). Expression of CD5 was detected by an anti-human CD5-specific antibody (Abclonal, A6882). Expression of CD30 antigen was detected by an anti-human CD30 antibody (rabbit anti-CD30 polyclonal antibody, Bioss, bs-2495R). The His tag protein antibody was used with an anti-His antibody (Proteintech, 66005-1-Ig).

Isolation and culture of primary human T lymphocytes

Peripheral blood mononuclear cells (PBMCs) were extracted from anonymous blood specimens from healthy blood donors (Guangzhou Blood Center) using the Ficoll-Hypaque gradient separation method.

Figure 6. Nb-derived CD30 and CD5 bispecific CAR-T cells enhanced anti-tumor potency *in vivo*

(A) Fluorescence-activated cell sorting (FACS) analysis shows the proportion of tumor-infiltrating CAR-T cells and cytokine production capacity. (B) Immunofluorescence staining of tumor tissue sections. The tumor tissue sections were analyzed for immunofluorescence by staining with anti-human CD8 (red), anti-human IFN-γ (green), and anti-human granzyme B (pink) antibodies, and the nuclei were stained with DAPI (blue). The statistical plot shows the mean fluorescence intensity statistics for CD8, IFN-γ, and granzyme B expressed as the mean ± SD from three randomly selected fields of thin tumor sections. Scale bar, 20 μm. (C) Survival curve of mice after tumor inoculation and then injection of the indicated CAR-T cells. *$p < 0.05$, **$p < 0.01$, log rank Mantel-Cox test. All data are mean ± standard error; *$p < 0.05$, **$p < 0.01$, ***$p < 0.001$, ****$p < 0.0001$, one-way ANOVA.

Primary human $CD8^+$ T cells were purified by negatively selected magnetic beads (BD Biosciences) with greater than 98% purity by enrichment set (BD-IMag). T lymphocytes were activated with 1 μg/mL of anti-CD3 and anti-CD28 antibodies (STEMCELL Technologies). T cells were cultured in lymphocyte serum-free medium (KBM581, Corning; initial concentration of 1×10^6 cells/mL). The cells were supplemented with recombinant IL-2 (10 ng/mL^{-1}; R&D Systems) twice a week.

Transduction of recombinant lentiviral particles

One day before transduction, the culture dishes were pretreated with poly-L-lysine, and HEK293T cells in 10-cm dishes and were spread evenly at a 1:4 ratio. 24 h later, after observing that the cell density reached 80%, HEK293T cells were treated with Opti-MEM medium (1 mL corresponding to one 10-cm dish) with Polyethylenimine (PEI)-three plasmids mixture, three plasmids contain CAR plasmid encoding CAR fragments (10 μg), pMD.2 G plasmid encoding the vesicular stomatitis virus G protein (VSV-G) envelope (4 μg) and packaging vector plasmid psPAX2 (10 μg) for co-transfection, using the PEI transfection system (PEI MAX transfection-grade linear polyethylenimine hydrochloride, molecular weight [MW] 40,000, Polysciences). 8–12 h later, successful transfection could be observed under fluorescence microscopy while replacing 10 mL of fresh medium. 48 h later, the supernatant was collected, and cell debris was removed by filtration with a 0.45-μm membrane. 10 mL of virus solution was added to a 50-mL centrifuge tube and then concentrated by adding virus concentration reagent (3 mL 50% Polyethylene glycol (PEG) 6000 + 1.28 mL 4 mol/L NaCl + 1.37 mL PBS) and then mixed well and placed in a refrigerator at 4°C overnight. The activated $CD8^+$ T lymphocytes were then transduced with 8 μg mL^{-1} Polybrene (TR-1003-G, Sigma)-coated lentiviral suspension, centrifuged at $350 \times g$ for 90 min, and incubated at 37°C. After 12 h, the recombinant virus was removed, and T cells were expanded in the conditioned medium. Transgenic T cells were maintained in complete T cell medium in the presence of IL-2 (fed twice weekly at 10 ng mL^{-1}).

Cytotoxicity assay

The specific killing activity of T cells toward tumors at different E:T ratios was measured after co-culture for 8 days by lactate dehydrogenase assay using the CytoTox 96 Nonradioactive Cytotoxicity Kit (G1781, Promega). The manufacturer's instructions were followed. Absorbance values of wells containing effector cells alone and target cells alone were combined and subtracted as background from the values of the co-cultures. Wells containing target cells alone were mixed with a lysis reagent for 30 min at 37°C, and the resulting luminescence was set as 100% lysis. Cytotoxicity was calculated using the following formula: %cytotoxicity = (experimental – effector spontaneous – target spontaneous) / (target maximum – target spontaneous) × 100%.

ELISA

Various CAR-T cells were co-cultured with target cells in 96-well plates (V bottom) at 10:1 (E:T ratio). Supernatants were collected after 24 h and analyzed for cytokine release using human IFN-γ, TNF-α, IL-2, and granzyme B-specific cytokine ELISA kits (DAKEWE) according to the manufacturer's instructions.

Enzyme-linked immunosorbent spot assay

In the enzyme-linked immunosorbent spot (ELISpot) assay, CAR-T cells were mixed with target cells (10^4 cells) at an E:T ratio of 10:1) and then added to an anti-human IFN-γ antibody prepackaged plate from the Human IFN-γ ELISpot Assay Kit (DAKEWE) with a negative control (effector $CD8^+$ T cells alone). 24 h later, ELISpot assays were performed according to the manufacturer's instructions. Plates were scanned with the ImmunoSpot S6 scan reader (Cellular Technology), and the number of IFN-γ positive T cells was calculated using ImmunoSpot software (v.5.1.34) (Cellular Technology).

Flow cytometry

For target antigens staining, the following antibodies were used: mouse anti-human PE-CD30 (BD Biosciences, 550041) and mouse anti-human Brilliant Violet 421-CD5 (BD Biosciences, 562646). For T cell phenotype staining, the following antibodies were used for extracellular staining: mouse anti-human PE-CD3 (eBioscience, 12-0038-42) and mouse anti-human Brilliant Violet 421-CD8 (eBioscience, 404-0088-42). For intracellular staining, T cells were fixed and permeabilized using the BD Cytofix/Cytoperm Kit. Intracellular staining was performed using mouse anti-human fluorescein isothiocyanate (FITC)-IFN-γ (eBioscience, 11-7319-82), APC (allophycocyanin)-IL-2 (eBioscience, 17-7029-82), and AF647-granzyme-B (BioLegend, 396421). The phage flow cytometry procedure was as follows. Karpas-299 cells with high expression of CD30 and CD5 as positive target cells were incubated with monoclonal phages at room temperature for 30 min, and the His-tagged phages binding to antigen on the cell surface were labeled with His fluorescent antibody (anti-PE-His, Biolegend, 362603). Stained samples were collected by a BD FACSAria and analyzed using FlowJo software (Tree Star, Ashland, OR, USA).

Xenograft mouse model

We used NCG mice (non-obese diabetic [NOD]/ShiLtJGpt-Prkdc^{em26Cd52}Il2rg^{em26Cd22}/Gpt, GuangDong GemPharmatech) to evaluate the *in vivo* anti-tumor effects of transduced CAR-T cells. All mouse experiments were strictly ethical and approved by Sun Yat-sen University's institutional animal care and use Committee. 6×10^6 Karpas-299 cells were subcutaneously injected into 6- to 8-week-old NCG mice to observe their anti-tumor activity. The tumor volume (V = 1/2 × long diameter × short diameter^2) was measured by two-dimensional measurement after 7–10 days. When the tumor volume reached 100 mm^3, 3×10^6 transduced CAR-T cells (200 μL PBS) were transferred into tumor-bearing mice via the tail vein, and at the same time, the mice were given an intraperitoneal injection of IL-2 at a dose of 1–2 μg per mouse every 2–3 days. The dynamic growth of tumors in each group was monitored (tumor volume and survival status). Three weeks after the CAR-T cell infusion, mice were executed, and the tumor tissues were separated for subsequent experiments. Some tumor tissues were digested with collagenase type IV (2 mg mL^{-1}, Sigma) at 37°C for 30 min, and tumor-infiltrating

T cells were isolated by discontinuous Percoll gradient centrifugation (Hao Yang, China) for subsequent analysis.

Immunohistochemistry and immunofluorescence

Tissue samples were fixed, treated, and stained according to standard procedures. Simply, the tumor was excised from mice, fixed with 4% neutral buffer formaldehyde, and embedded in paraffin at the Institute of Biopathology (Servicebio, China). The primary antibodies used for immunohistochemistry staining were a rabbit anti-human CD3 monoclonal antibody (176171-AP, Proteintech) and a rabbit anti-human IFN-γ monoclonal antibody (ab9657, Abcam). Immunohistochemistry (IHC) section images were obtained using a microscope (Leica, DM6000B). The primary antibodies used for immunofluorescence staining were as follows: rabbit anti-human CD8 antibody (GB13068, Servicebio), rabbit anti-human IFN-γ antibody (GB11107-1, Servicebio), and mouse anti-human GZMB antibody (GB14092, Servicebio). Fluorescent secondary antibodies were as follows: goat anti-rabbit antibody labeled with horseradish peroxidase (HRP; GB23303, Servicebio), goat anti-mouse antibody labeled with HRP (GB23301, Servicebio), and goat anti-mouse antibody labeled with CY5 (GB27301, Servicebio). DAPI (G1012, Servicebio) was used for staining of the nucleus. Pathological section scanners (Pannoramic, 3Dhistech) were used to detect fluorescence signals. To quantify the immunofluorescence results, the average fluorescence intensity was analyzed using ImageJ software.

Eukaryotic expression and purification of proteins (antigen proteins and antibody-Fc proteins)

The CD30 and CD5 antigen extracellular domains were amplified from the Karpas cell cDNA by PCR and cloned into the pcDNA3.1 expression vector ligated with the His tag. The CD30 and CD5 expression plasmid was transfected into HEK293F cells with PEI reagent. Cells were then given the supplement reagent (Chinese hamster ovary [CHO] PFF05, Shanghai OPM Biosciences Co., Ltd) twice after 24 h and after 96 h. About 7 days after transfection, the supernatant of the cell culture was collected. The supernatants were incubated with Ni-NTA (Nitrilotriacetic acid) agarose (Cytiva) to enrich His-tagged CD30 and CD5 antigen extracellular domain proteins, followed by protein elution with Tris-NaCl buffer containing imidazole. The concentration of protein was determined by BCA assay. The scFv -Fc or Nb-Fc fragments were cloned into the pcDNA3.1 expression vector. After transfection into HEK293F cells, the culture supernatant was purified and concentrated by protein A, and the scFv/Nb-Fc protein was used for subsequent ELISA experiments.

Immunization of alpacas and construction of an Nb library

Two healthy 2-year-old alpacas were injected subcutaneously, with the extracellular domain of CD30 and CD5 protein (1 mg in PBS) mixed with adjuvant, at 2-week intervals four times. Eight weeks later, PBMCs were collected, the total RNA was extracted, and cDNA was synthesized by reverse transcription kit. The VHHs were amplified by two rounds of PCR with the designed antibody amplification specific primers. The PCR product were digested with sfiI restriction enzymes and ligated into the pComb3XSS vector. Then the vector was electroporated into *E. coli* SS320 electrocompetent cells. The resulting SS320 library stock was then infected with M13K07 helper phages to obtain a library of VHH-presenting phages.

Phage library screening of CD30 and CD5 Nbs

Nbs against CD30 or CD5 were screened by phage display. The purified and concentrated phage library was incubated with purified CD5 or CD30 in an immune tube (12-1275, BIOLOGIX). After incubation, phages without binding antigen were washed with PBS, the binding phages were eluted with trypsin, and the eluted phages were purified and amplified. Phage titers were tested after each screening. After 3 rounds of repeated screening, positive phage clones were selected for phage amplification and purification.

Monoclonal phage ELISA

The CD30 or CD5 antigen proteins were coated onto 96-well microtiter plates in coating buffer overnight at 4°C and blocked with 3% BSA for 1 h at 37°C. The coated plates were incubated with different positive purified monoclonal phages for 1 h at 37°C and, subsequently, with mouse annti-M13 monoclonal antibody (HRP) (Sino Biological, Beijing, China) for 1 h at 37°C. Each incubation was followed by four washes with PBS-T (PBS-tween-20). Finally, TMB (3,3',5,5'-Tetramethylbenzidine) substrate (Invitrogen, Thermo Fisher Scientific) was added, and absorption was measured at 450 nm.

scFv/Nb-Fc antibody ELISA

The CD30 or CD5 antigen proteins were coated onto 96-well microtiter plates in coating buffer overnight at 4°C and blocked with 3% BSA for 1 h at 37°C. The coated plates were incubated with Nb-Fc or scFv-Fc for 1 h at 37°C and, subsequently, with goat anti-human IgG-Fc secondary antibody (HRP) (Sino Biological) for 1 h at 37°C. Each incubation was followed by four washes with PBS-T. Finally, TMB substrate (Invitrogen, Thermo Fisher Scientific) was added, and absorption was measured at 450 nm.

Prediction of antigen-antibody binding capacity

Molecular docking of antigen-antibody binding was performed by predicting antibody protein 3D structure models as a basis. A protein structure prediction website (Protein Homology/analogY Recognition Engine v.2.0) was used to predict the 3D structures of Nb-Fc and scFv-Fc, and the 3D structures of CD30 and CD5 antigen proteins were obtained from the AlphaFold Protein Structure Database. The prediction model of the binding between the antigen and corresponding antibody was obtained using the ZDOCK (a rigid-body docking algorithm) molecular docking website.

Surface plasmon resonance (SPR)

The antibody-antigen interaction was measured with a BIAcore T100 instrument (Cytiva). The CM5 sensor chip (Cytiva) was activated and then injected with CD5-His or CD30-His protein at a suitable pH value of 4.5–5.5 for immobilization (1.5–5 μg/mL in 10 mM acetate buffer) into channels 2 and 4. The remaining activated groups on the chip were blocked by injecting ethanolamine HCl (1 M). The binding status of CD5-His or CD30-His to antibody were monitored

at different concentrations for about 4 min. The dissociation time of the antibody in each cycle was 20–25 min. The calculation of K_D was measured by the association constant (K_A) and diffusion constant (K_d).

Statistical analysis

Statistical tests were conducted using Prism (GraphPad) software. All experimental data are presented as mean ± SEM. A t test was used for comparison of two sample means, and one-way ANOVA was used for comparison of multiple groups' means; $p < 0.05$ was considered statistically significant.

DATA AND CODE AVAILABILITY

All data needed to evaluate the conclusions in the paper are present in the paper and/or the supplemental information.

SUPPLEMENTAL INFORMATION

Supplemental information can be found online at https://doi.org/10.1016/j.omto.2023.07.007.

ACKNOWLEDGMENTS

This work was supported by Important Key Program of the Talent research funding of Guangdong Provincial People's Hospital (KJ012019376), the Natural Science Foundation of China (NSFC) (81730060 and 92169201), the Exchange Program of NSFC (82150710553), and the Special Research and Development Program of Guangzhou (202008070010) (to H.Z.); the National Key Research and Development Program (2021YFC2301904 to B.L.); the Guangdong Province High-level Hospital Construction Project of Guangdong Provincial People's Hospital, Guangdong Academy of Medical Sciences (DFJH2020025 to W.L.; the Natural Science Foundation of China (82072265 to L. Li); the Guangdong Basic and Applied Basic Research Foundation (2023A1515010476 to C.C.); the Basic and Applied Basic Research Fund Committee of Guangdong Province (21201910240000200) and National Natural Science Foundation of China (82202036) (to L. Lu); and the National Natural Science Foundation of China (NSFC; 82171825 and 32100743) (to X.H.).

AUTHOR CONTRIBUTIONS

B.X. designed the experiments, performed most of these experiments, analyzed the data, and wrote the manuscript. K.L., X.W., F.C., M.Z., Y. Li, Y. Lin, Y.Q., R.L., and W.Z. made substantial contributions to the acquisition of data and data analyses. X.H., F.Z., and L. Li provided scientific expertise and supervised analysis of clinical experience. W.L., B.L., and H.Z. have full access to all data in the study and take responsibility for the integrity of the data and the accuracy of the data analysis. All authors reviewed and approved the final version of the report.

DECLARATION OF INTERESTS

The authors declare no competing interests.

REFERENCES

1. Cazzola, M. (2016). Introduction to a review series: the 2016 revision of the WHO classification of tumors of hematopoietic and lymphoid tissues. Blood *127*, 2361–2364. https://doi.org/10.1182/blood-2016-03-657379.

2. Chihara, D., Ito, H., Matsuda, T., Shibata, A., Katsumi, A., Nakamura, S., Tomotaka, S., Morton, L.M., Weisenburger, D.D., and Matsuo, K. (2014). Differences in incidence and trends of haematological malignancies in Japan and the United States. Br. J. Haematol. *164*, 536–545. https://doi.org/10.1111/bjh.12659.

3. Teras, L.R., DeSantis, C.E., Cerhan, J.R., Morton, L.M., Jemal, A., and Flowers, C.R. (2016). 2016 US lymphoid malignancy statistics by World Health Organization subtypes. CA. Cancer J. Clin. *66*, 443–459. https://doi.org/10.3322/caac.21357.

4. Bellei, M., Foss, F.M., Shustov, A.R., Horwitz, S.M., Marcheselli, L., Kim, W.S., Cabrera, M.E., Dlouhy, I., Nagler, A., Advani, R.H., et al.; International T-cell Project Network (2018). The outcome of peripheral T-cell lymphoma patients failing first-line therapy: a report from the prospective, International T-Cell Project. Haematologica *103*, 1191–1197. https://doi.org/10.3324/haematol.2017.186577.

5. Chihara, D., Fanale, M.A., Miranda, R.N., Noorani, M., Westin, J.R., Nastoupil, L.J., Hagemeister, F.B., Fayad, L.E., Romaguera, J.E., Samaniego, F., et al. (2017). The survival outcome of patients with relapsed/refractory peripheral T-cell lymphoma-not otherwise specified and angioimmunoblastic T-cell lymphoma. Br. J. Haematol. *176*, 750–758. https://doi.org/10.1111/bjh.14477.

6. Ellin, F., Landström, J., Jerkeman, M., and Relander, T. (2014). Real-world data on prognostic factors and treatment in peripheral T-cell lymphomas: a study from the Swedish Lymphoma Registry. Blood *124*, 1570–1577. https://doi.org/10.1182/blood-2014-04-573089.

7. Mak, V., Hamm, J., Chhanabhai, M., Shenkier, T., Klasa, R., Sehn, L.H., Villa, D., Gascoyne, R.D., Connors, J.M., and Savage, K.J. (2013). Survival of patients with peripheral T-cell lymphoma after first relapse or progression: spectrum of disease and rare long-term survivors. J. Clin. Oncol. *31*, 1970–1976. https://doi.org/10.1200/jco.2012.44.7524.

8. Fiore, D., Cappelli, L.V., Broccoli, A., Zinzani, P.L., Chan, W.C., and Inghirami, G. (2020). Peripheral T cell lymphomas: from the bench to the clinic. Nat. Rev. Cancer *20*, 323–342. https://doi.org/10.1038/s41568-020-0247-0.

9. Chihara, D., Miljkovic, M., Iyer, S.P., and Vega, F. (2021). Targeted based therapy in nodal T-cell lymphomas. Leukemia *35*, 956–967. https://doi.org/10.1038/s41375-021-01191-8.

10. Iżykowska, K., Rassek, K., Korsak, D., and Przybylski, G.K. (2020). Novel targeted therapies of T cell lymphomas. J. Hematol. Oncol. *13*, 176. https://doi.org/10.1186/s13045-020-01006-w.

11. Gross, G., Waks, T., and Eshhar, Z. (1989). Expression of immunoglobulin-T-cell receptor chimeric molecules as functional receptors with antibody-type specificity. Proc. Natl. Acad. Sci. USA *86*, 10024–10028. https://doi.org/10.1073/pnas.86.24.10024.

12. Ramello, M.C., Benzaïd, I., Kuenzi, B.M., Lienlaf-Moreno, M., Kandell, W.M., Santiago, D.N., Pabón-Saldaña, M., Darville, L., Fang, B., Rix, U., et al. (2019). An immunoproteomic approach to characterize the CAR interactome and signalosome. Sci. Signal. *12*, eaap9777. https://doi.org/10.1126/scisignal.aap9777.

13. Maude, S.L., Frey, N., Shaw, P.A., Aplenc, R., Barrett, D.M., Bunin, N.J., Chew, A., Gonzalez, V.E., Zheng, Z., Lacey, S.F., et al. (2014). Chimeric antigen receptor T cells for sustained remissions in leukemia. N. Engl. J. Med. *371*, 1507–1517. https://doi.org/10.1056/NEJMoa1407222.

14. Kochenderfer, J.N., Wilson, W.H., Janik, J.E., Dudley, M.E., Stetler-Stevenson, M., Feldman, S.A., Maric, I., Raffeld, M., Nathan, D.A.N., Lanier, B.J., et al. (2010). Eradication of B-lineage cells and regression of lymphoma in a patient treated with autologous T cells genetically engineered to recognize CD19. Blood *116*, 4099–4102. https://doi.org/10.1182/blood-2010-04-281931.

15. Wang, Y., Zhang, W.Y., Han, Q.W., Liu, Y., Dai, H.R., Guo, Y.L., Bo, J., Fan, H., Zhang, Y., Zhang, Y.J., et al. (2014). Effective response and delayed toxicities of refractory advanced diffuse large B-cell lymphoma treated by CD20-directed chimeric antigen receptor-modified T cells. Clin. Immunol. *155*, 160–175. https://doi.org/10.1016/j.clim.2014.10.002.

16. Buckley, R.H., Schiff, S.E., Schiff, R.I., Markert, L., Williams, L.W., Roberts, J.L., Myers, L.A., and Ward, F.E. (1999). Hematopoietic stem-cell transplantation for

the treatment of severe combined immunodeficiency. N. Engl. J. Med. *340*, 508–516. https://doi.org/10.1056/nejm199902183400703.

17. Leonard, W.J. (2001). Cytokines and immunodeficiency diseases. Nat. Rev. Immunol. *1*, 200–208. https://doi.org/10.1038/35105066.

18. Went, P., Agostinelli, C., Gallamini, A., Piccaluga, P.P., Ascani, S., Sabattini, E., Bacci, F., Falini, B., Motta, T., Paulli, M., et al. (2006). Marker expression in peripheral T-cell lymphoma: a proposed clinical-pathologic prognostic score. J. Clin. Oncol. *24*, 2472–2479. https://doi.org/10.1200/jco.2005.03.6327.

19. d'Amore, F., Gaulard, P., Trümper, L., Corradini, P., Kim, W.S., Specht, L., Bjerregaard Pedersen, M., and Ladetto, M.; ESMO Guidelines Committee (2015). Peripheral T-cell lymphomas: ESMO Clinical Practice Guidelines for diagnosis, treatment and follow-up. Ann. Oncol. *26*, v108–v115. https://doi.org/10.1093/annonc/mdv201.

20. Mamonkin, M., Rouce, R.H., Tashiro, H., and Brenner, M.K. (2015). A T-cell-directed chimeric antigen receptor for the selective treatment of T-cell malignancies. Blood *126*, 983–992. https://doi.org/10.1182/blood-2015-02-629527.

21. Pinz, K., Liu, H., Golightly, M., Jares, A., Lan, F., Zieve, G.W., Hagag, N., Schuster, M., Firor, A.E., Jiang, X., and Ma, Y. (2016). Preclinical targeting of human T-cell malignancies using CD4-specific chimeric antigen receptor (CAR)-engineered T cells. Leukemia *30*, 701–707. https://doi.org/10.1038/leu.2015.311.

22. Ramos, C.A., Ballard, B., Zhang, H., Dakhova, O., Gee, A.P., Mei, Z., Bilgi, M., Wu, M.F., Liu, H., Grilley, B., et al. (2017). Clinical and immunological responses after CD30-specific chimeric antigen receptor-redirected lymphocytes. J. Clin. Invest. *127*, 3462–3471. https://doi.org/10.1172/jci94306.

23. Wang, C.M., Wu, Z.Q., Wang, Y., Guo, Y.L., Dai, H.R., Wang, X.H., Li, X., Zhang, Y.J., Zhang, W.Y., Chen, M.X., et al. (2017). Autologous T Cells Expressing CD30 Chimeric Antigen Receptors for Relapsed or Refractory Hodgkin Lymphoma: An Open-Label Phase I Trial. Clin. Cancer Res. *23*, 1156–1166. https://doi.org/10.1158/1078-0432.Ccr-16-1365.

24. Lu, X., Axtell, R.C., Collawn, J.F., Gibson, A., Justement, L.B., and Raman, C. (2002). AP2 adaptor complex-dependent internalization of CD5: differential regulation in T and B cells. J. Immunol. *168*, 5612–5620. https://doi.org/10.4049/jimmunol.168.11.5612.

25. Falini, B., Pileri, S., Pizzolo, G., Dürkop, H., Flenghi, L., Stirpe, F., Martelli, M.F., and Stein, H. (1995). CD30 (Ki-1) molecule: a new cytokine receptor of the tumor necrosis factor receptor superfamily as a tool for diagnosis and immunotherapy. Blood *85*, 1–14.

26. Zheng, W., Medeiros, L.J., Young, K.H., Goswami, M., Powers, L., Kantarjian, H.H., Thomas, D.A., Cortes, J.E., and Wang, S.A. (2014). CD30 expression in acute lymphoblastic leukemia as assessed by flow cytometry analysis. Leuk. Lymphoma *55*, 624–627. https://doi.org/10.3109/10428194.2013.820293.

27. Savoldo, B., Rooney, C.M., Di Stasi, A., Abken, H., Hombach, A., Foster, A.E., Zhang, L., Heslop, H.E., Brenner, M.K., and Dotti, G. (2007). Epstein Barr virus specific cytotoxic T lymphocytes expressing the anti-CD30zeta artificial chimeric T-cell receptor for immunotherapy of Hodgkin disease. Blood *110*, 2620–2630. https://doi.org/10.1182/blood-2006-11-059139.

28. de Claro, R.A., McGinn, K., Kwitkowski, V., Bullock, J., Khandelwal, A., Habtemariam, B., Ouyang, Y., Saber, H., Lee, K., Koti, K., et al. (2012). U.S. Food and Drug Administration approval summary: brentuximab vedotin for the treatment of relapsed Hodgkin lymphoma or relapsed systemic anaplastic large-cell lymphoma. Clin. Cancer Res. *18*, 5845–5849. https://doi.org/10.1158/1078-0432.Ccr-12-1803.

29. Braig, F., Brandt, A., Goebeler, M., Tony, H.P., Kurze, A.K., Nollau, P., Bumm, T., Böttcher, S., Bargou, R.C., and Binder, M. (2017). Resistance to anti-CD19/CD3 BiTE in acute lymphoblastic leukemia may be mediated by disrupted CD19 membrane trafficking. Blood *129*, 100–104. https://doi.org/10.1182/blood-2016-05-718395.

30. Ruella, M., Barrett, D.M., Kenderian, S.S., Shestova, O., Hofmann, T.J., Perazzelli, J., Klichinsky, M., Aikawa, V., Nazimuddin, F., Kozlowski, M., et al. (2016). Dual CD19 and CD123 targeting prevents antigen-loss relapses after CD19-directed immunotherapies. J. Clin. Invest. *126*, 3814–3826. https://doi.org/10.1172/jci87366.

31. Jia, H., Wang, Z., Wang, Y., Liu, Y., Dai, H., Tong, C., Guo, Y., Guo, B., Ti, D., Han, X., et al. (2019). Haploidentical CD19/CD22 bispecific CAR-T cells induced MRD-negative remission in a patient with relapsed and refractory adult B-ALL after haploidentical hematopoietic stem cell transplantation. J. Hematol. Oncol. *12*, 57. https://doi.org/10.1186/s13045-019-0741-6.

32. Tong, C., Zhang, Y., Liu, Y., Ji, X., Zhang, W., Guo, Y., Han, X., Ti, D., Dai, H., Wang, C., et al. (2020). Optimized tandem CD19/CD20 CAR-engineered T cells in refractory/relapsed B-cell lymphoma. Blood *136*, 1632–1644. https://doi.org/10.1182/blood.2020005278.

33. Hamers-Casterman, C., Atarhouch, T., Muyldermans, S., Robinson, G., Hamers, C., Songa, E.B., Bendahman, N., and Hamers, R. (1993). Naturally occurring antibodies devoid of light chains. Nature *363*, 446–448. https://doi.org/10.1038/363446a0.

34. Harmsen, M.M., Ruuls, R.C., Nijman, I.J., Niewold, T.A., Frenken, L.G., and de Geus, B. (2000). Llama heavy-chain V regions consist of at least four distinct subfamilies revealing novel sequence features. Mol. Immunol. *37*, 579–590. https://doi.org/10.1016/s0161-5890(00)00081-x.

35. Verhaar, E.R., Woodham, A.W., and Ploegh, H.L. (2021). Nanobodies in cancer. Semin. Immunol. *52*, 101425. https://doi.org/10.1016/j.smim.2020.101425.

36. Bao, G., Tang, M., Zhao, J., and Zhu, X. (2021). Nanobody: a promising toolkit for molecular imaging and disease therapy. EJNMMI Res. *11*, 6. https://doi.org/10.1186/s13550-021-00750-5.

37. Salvador, J.P., Vilaplana, L., and Marco, M.P. (2019). Nanobody: outstanding features for diagnostic and therapeutic applications. Anal. Bioanal. Chem. *411*, 1703–1713. https://doi.org/10.1007/s00216-019-01633-4.

38. Unciti-Broceta, J.D., Del Castillo, T., Soriano, M., Magez, S., and Garcia-Salcedo, J.A. (2013). Novel therapy based on camelid nanobodies. Ther. Deliv. *4*, 1321–1336. https://doi.org/10.4155/tde.13.87.

39. Xie, Y.J., Dougan, M., Ingram, J.R., Pishesha, N., Fang, T., Momin, N., and Ploegh, H.L. (2020). Improved Antitumor Efficacy of Chimeric Antigen Receptor T Cells that Secrete Single-Domain Antibody Fragments. Cancer Immunol. Res. *8*, 518–529. https://doi.org/10.1158/2326-6066.Cir-19-0734.

40. Sharifzadeh, Z., Rahbarizadeh, F., Shokrgozar, M.A., Ahmadvand, D., Mahboudi, F., Jamnani, F.R., and Moghimi, S.M. (2013). Genetically engineered T cells bearing chimeric nanoconstructed receptors harboring TAG-72-specific camelid single domain antibodies as targeting agents. Cancer Lett. *334*, 237–244. https://doi.org/10.1016/j.canlet.2012.08.010.

41. De Munter, S., Van Parys, A., Bral, L., Ingels, J., Goetgeluk, G., Bonte, S., Pille, M., Billiet, L., Weening, K., Verhee, A., et al. (2020). Rapid and Effective Generation of Nanobody Based CARs using PCR and Gibson Assembly. Int. J. Mol. Sci. *21*, 883. https://doi.org/10.3390/ijms21030883.

42. He, X., Feng, Z., Ma, J., Ling, S., Cao, Y., Gurung, B., Wu, Y., Katona, B.W., O'Dwyer, K.P., Siegel, D.L., et al. (2020). Bispecific and split CAR T cells targeting CD13 and TIM3 eradicate acute myeloid leukemia. Blood *135*, 713–723. https://doi.org/10.1182/blood.2019002779.

43. Zhao, W.H., Liu, J., Wang, B.Y., Chen, Y.X., Cao, X.M., Yang, Y., Zhang, Y.L., Wang, F.X., Zhang, P.Y., Lei, B., et al. (2018). A phase 1, open-label study of LCAR-B38M, a chimeric antigen receptor T cell therapy directed against B cell maturation antigen, in patients with relapsed or refractory multiple myeloma. J. Hematol. Oncol. *11*, 141. https://doi.org/10.1186/s13045-018-0681-6.

44. Loh, B., Haase, M., Mueller, L., Kuhn, A., and Leptihn, S. (2017). The Transmembrane Morphogenesis Protein gp1 of Filamentous Phages Contains Walker A and Walker B Motifs Essential for Phage Assembly. Viruses *9*. https://doi.org/10.3390/v9040073.

45. Chowdhury, P.S., Viner, J.L., Beers, R., and Pastan, I. (1998). Isolation of a high-affinity stable single-chain Fv specific for mesothelin from DNA-immunized mice by phage display and construction of a recombinant immunotoxin with anti-tumor activity. Proc. Natl. Acad. Sci. USA *95*, 669–674. https://doi.org/10.1073/pnas.95.2.669.

46. Silence, K., Dreier, T., Moshir, M., Ulrichts, P., Gabriels, S.M.E., Saunders, M., Wajant, H., Brouckaert, P., Huyghe, L., Van Hauwermeiren, T., et al. (2014). ARGX-110, a highly potent antibody targeting CD70, eliminates tumors via both enhanced ADCC and immune checkpoint blockade. mAbs *6*, 523–532. https://doi.org/10.4161/mabs.27398.

47. Studnicka, G.M., Soares, S., Better, M., Williams, R.E., Nadell, R., and Horwitz, A.H. (1994). Human-engineered monoclonal antibodies retain full specific binding activity by preserving non-CDR complementarity-modulating residues. Protein Eng. *7*, 805–814. https://doi.org/10.1093/protein/7.6.805.

48. Zhao, L., Li, S., Wei, X., Qi, X., Liu, D., Liu, L., Wen, F., Zhang, J.S., Wang, F., Liu, Z.L., and Cao, Y.J. (2022). A novel CD19/CD22/CD3 trispecific antibody enhances therapeutic efficacy and overcomes immune escape against B-ALL. Blood *140*, 1790–1802. https://doi.org/10.1182/blood.2022016243.

49. Dai, Z., Mu, W., Zhao, Y., Cheng, J., Lin, H., Ouyang, K., Jia, X., Liu, J., Wei, Q., Wang, M., et al. (2022). T cells expressing CD5/CD7 bispecific chimeric antigen receptors with fully human heavy-chain-only domains mitigate tumor antigen escape. Signal Transduct. Target. Ther. *7*, 85. https://doi.org/10.1038/s41392-022-00898-z.

50. Liu, B., Zou, F., Lu, L., Chen, C., He, D., Zhang, X., Tang, X., Liu, C., Li, L., and Zhang, H. (2016). Chimeric Antigen Receptor T Cells Guided by the Single-Chain Fv of a Broadly Neutralizing Antibody Specifically and Effectively Eradicate Virus Reactivated from Latency in CD4+ T Lymphocytes Isolated from HIV-1-Infected Individuals Receiving Suppressive Combined Antiretroviral Therapy. J. Virol. *90*, 9712–9724. https://doi.org/10.1128/jvi.00852-16.

51. Zou, F., Lu, L., Liu, J., Xia, B., Zhang, W., Hu, Q., Liu, W., Zhang, Y., Lin, Y., Jing, S., et al. (2019). Engineered triple inhibitory receptor resistance improves anti-tumor CAR-T cell performance via CD56. Nat. Commun. *10*, 4109. https://doi.org/10.1038/s41467-019-11893-4.

52. O'Connor, O.A., Pro, B., Pinter-Brown, L., Bartlett, N., Popplewell, L., Coiffier, B., Lechowicz, M.J., Savage, K.J., Shustov, A.R., Gisselbrecht, C., et al. (2011). Pralatrexate in patients with relapsed or refractory peripheral T-cell lymphoma: results from the pivotal PROPEL study. J. Clin. Oncol. *29*, 1182–1189. https://doi.org/10.1200/jco.2010.29.9024.

53. Coiffier, B., Pro, B., Prince, H.M., Foss, F., Sokol, L., Greenwood, M., Caballero, D., Borchmann, P., Morschhauser, F., Wilhelm, M., et al. (2012). Results from a pivotal, open-label, phase II study of romidepsin in relapsed or refractory peripheral T-cell lymphoma after prior systemic therapy. J. Clin. Oncol. *30*, 631–636. https://doi.org/10.1200/jco.2011.37.4223.

54. Pro, B., Advani, R., Brice, P., Bartlett, N.L., Rosenblatt, J.D., Illidge, T., Matous, J., Ramchandren, R., Fanale, M., Connors, J.M., et al. (2012). Brentuximab vedotin (SGN-35) in patients with relapsed or refractory systemic anaplastic large-cell lymphoma: results of a phase II study. J. Clin. Oncol. *30*, 2190–2196. https://doi.org/10.1200/jco.2011.38.0402.

55. O'Connor, O.A., Horwitz, S., Masszi, T., Van Hoof, A., Brown, P., Doorduijn, J., Hess, G., Jurczak, W., Knoblauch, P., Chawla, S., et al. (2015). Belinostat in Patients With Relapsed or Refractory Peripheral T-Cell Lymphoma: Results of the Pivotal Phase II BELIEF (CLN-19) Study. J. Clin. Oncol. *33*, 2492–2499. https://doi.org/10.1200/jco.2014.59.2782.

56. Sadelain, M., Brentjens, R., and Rivière, I. (2013). The basic principles of chimeric antigen receptor design. Cancer Discov. *3*, 388–398. https://doi.org/10.1158/2159-8290.Cd-12-0548.

57. Dhodapkar, M.V., and Richter, J. (2011). Harnessing natural killer T (NKT) cells in human myeloma: progress and challenges. Clin. Immunol. *140*, 160–166. https://doi.org/10.1016/j.clim.2010.12.010.

58. Zah, E., Lin, M.Y., Silva-Benedict, A., Jensen, M.C., and Chen, Y.Y. (2016). T Cells Expressing CD19/CD20 Bispecific Chimeric Antigen Receptors Prevent Antigen Escape by Malignant B Cells. Cancer Immunol. Res. *4*, 498–508. https://doi.org/10.1158/2326-6066.Cir-15-0231.

59. Kalos, M., and June, C.H. (2013). Adoptive T cell transfer for cancer immunotherapy in the era of synthetic biology. Immunity *39*, 49–60. https://doi.org/10.1016/j.immuni.2013.07.002.

60. Pemmaraju, N. (2017). Novel Pathways and Potential Therapeutic Strategies for Blastic Plasmacytoid Dendritic Cell Neoplasm (BPDCN): CD123 and Beyond. Curr. Hematol. Malig. Rep. *12*, 510–512. https://doi.org/10.1007/s11899-017-0425-7.

61. Gomes-Silva, D., Srinivasan, M., Sharma, S., Lee, C.M., Wagner, D.L., Davis, T.H., Rouce, R.H., Bao, G., Brenner, M.K., and Mamonkin, M. (2017). CD7-edited T cells expressing a CD7-specific CAR for the therapy of T-cell malignancies. Blood *130*, 285–296. https://doi.org/10.1182/blood-2017-01-761320.

62. Cooper, M.L., Choi, J., Staser, K., Ritchey, J.K., Devenport, J.M., Eckardt, K., Rettig, M.P., Wang, B., Eissenberg, L.G., Ghobadi, A., et al. (2018). An "off-the-shelf" fratricide-resistant CAR-T for the treatment of T cell hematologic malignancies. Leukemia *32*, 1970–1983. https://doi.org/10.1038/s41375-018-0065-5.

63. Perera, L.P., Zhang, M., Nakagawa, M., Petrus, M.N., Maeda, M., Kadin, M.E., Waldmann, T.A., and Perera, P.Y. (2017). Chimeric antigen receptor modified T cells that target chemokine receptor CCR4 as a therapeutic modality for T-cell malignancies. Am. J. Hematol. *92*, 892–901. https://doi.org/10.1002/ajh.24794.

64. Kijanka, M., Dorresteijn, B., Oliveira, S., and van Bergen en Henegouwen, P.M.P. (2015). Nanobody-based cancer therapy of solid tumors. Nanomedicine (London, England) *10*, 161–174. https://doi.org/10.2217/nnm.14.178.

65. Arbabi Ghahroudi, M., Desmyter, A., Wyns, L., Hamers, R., and Muyldermans, S. (1997). Selection and identification of single domain antibody fragments from camel heavy-chain antibodies. FEBS Lett. *414*, 521–526. https://doi.org/10.1016/s0014-5793(97)01062-4.

66. Pérez, J.M., Renisio, J.G., Prompers, J.J., van Platerink, C.J., Cambillau, C., Darbon, H., and Frenken, L.G. (2001). Thermal unfolding of a llama antibody fragment: a two-state reversible process. Biochemistry *40*, 74–83. https://doi.org/10.1021/bi0009082.

67. Xie, Y.J., Dougan, M., Jailkhani, N., Ingram, J., Fang, T., Kummer, L., Momin, N., Pishesha, N., Rickelt, S., Hynes, R.O., and Ploegh, H. (2019). Nanobody-based CAR T cells that target the tumor microenvironment inhibit the growth of solid tumors in immunocompetent mice. Proc. Natl. Acad. Sci. USA *116*, 7624–7631. https://doi.org/10.1073/pnas.1817147116.

68. Mo, F., Duan, S., Jiang, X., Yang, X., Hou, X., Shi, W., Carlos, C.J.J., Liu, A., Yin, S., Wang, W., et al. (2021). Nanobody-based chimeric antigen receptor T cells designed by CRISPR/Cas9 technology for solid tumor immunotherapy. Signal Transduct. Target. Ther. *6*, 80. https://doi.org/10.1038/s41392-021-00462-1.

69. Nix, M.A., Mandal, K., Geng, H., Paranjape, N., Lin, Y.H.T., Rivera, J.M., Marcoulis, M., White, K.L., Whitman, J.D., Bapat, S.P., et al. (2021). Surface Proteomics Reveals CD72 as a Target for In Vitro-Evolved Nanobody-Based CAR-T Cells in KMT2A/MLL1-Rearranged B-ALL. Cancer Discov. *11*, 2032–2049. https://doi.org/10.1158/2159-8290.Cd-20-0242.

70. Zhang, M., Chen, D., Fu, X., Meng, H., Nan, F., Sun, Z., Yu, H., Zhang, L., Li, L., Li, X., et al. (2022). Autologous Nanobody-Derived Fratricide-Resistant CD7-CAR T-cell Therapy for Patients with Relapsed and Refractory T-cell Acute Lymphoblastic Leukemia/Lymphoma. Clin. Cancer Res. *28*, 2830–2843. https://doi.org/10.1158/1078-0432.Ccr-21-4097.